CONICAL FLOW MODELING FOR POLYGONAL CROSS SECTION BODIES AT OFF DESIGN CONDITIONS

BY

HAMID KAMKAR

B.Sc., University of Bristol

(1975)

SUBMITTED IN PARTIAL FULFILLMENT

OF THE REQUIREMENTS FOR THE

DEGREE OF MASTER OF SCIENCE

at the

MASSACHUSETTS INSTITUTE OF TECHNOLOGY

June, 1977

Signature of Author _____ Signature redacted

February 18, 1977

Certified by _____ Signature redacted

Thesis Supervisor

Accepted by _____ Signature redacted

Chairman, Departmental Graduate Committee

CONICAL FLOW MODELING FOR POLYGONAL CROSS SECTION BODIES AT OFF DESIGN CONDITIONS

by

HAMID KAMKAR

Submitted to the Department of Aeronautics and Astronautics on February 18, 1977 in partial fulfillment of the requirements for the degree of Master of Science.

ABSTRACT

A number of N-symmetric bodies with polygonal transverse sections are considered in a supersonic flow at zero angle of attack.

Due to nonlinearity of the conical field equation, the distribution of velocity components are approximated using equivalent cone distributions corresponding to a zero angle of attack, and in such a way as to satisfy all of the existing boundary conditions.

Depending on whether or not certain boundary conditions were satisfied on the symmetry lines, the problem was divided into three cases.

Case (1) for $\partial V_n/\partial\theta \neq 0$, i.e. a relaxation of the symmetry constraint, gave results which seemed to be unreasonable and inconsistent.

Case (2) for $\partial V_n/\partial\theta = 0$ was imposed on one symmetry line only, with the other (at $\theta = \pi/2$), represented as a flat plate at which $\partial V_n/\partial\theta \neq 0$. These results proved consistant and reasonable.

Finally, for case (3), $\partial V_n/\partial\theta = 0$ was imposed along both symmetry lines and introduced a singularity for velocity components.

The numerical results for this case were not included; however, an approach has been suggested to remove the singularity.

Thesis Supervisor: Judson R. Baron
Title: Professor of Aeronautics and Astronautics

ACKNOWLEDGEMENTS

I would like to thank Professor J.R. Baron for his patience and help during the time that I was working on this thesis. The general idea pursued in this work was due to Professor Baron.

Also, I would like to thank Mrs. Sherry Modestino for typing this thesis.

TABLE OF CONTENTS

Tables

Figures

Symbols

X,Y,Z	Cartesian coordinate axis
$\hat{i},\hat{j},\hat{k}$	Unit vectors in XYZ system
r,θ,σ	Spherical coordinate system
$\vec{V}_r$, $\vec{V}_n$, $\vec{W}$	Velocity vectors in spherical coordinates
$\hat{V}_r$, $\hat{V}_n$, $\hat{W}$	Unit vectors in direction of $\vec{V}_r$, $\vec{V}_n$, $\vec{W}$
V_r, V_n, W	Spherical velocity components
U_∞	Free stream velocity components
V_r', V_n', W'	Non-dimensionalized form of velocity components, $V_r' = V_r/U_\infty$
q_{max}	Maximum velocity = $(2C_pT_0)^{1/2}$
$\bar{V}_r$, $\bar{V}_n$, $\bar{W}$	Non-dimensionalized form of velocity components, $\bar{V}_r = V_r/q_{max}$, etc.
$\bar{W}_1$	Non-dimensionalized velocity for case (1) having sinusoidal dependence on θ
$\bar{V}_{n1}$	Non-dimensionalized velocity for case (1)
$\bar{W}_2$	Non-dimensionalized velocity for case (1) having partial sinusoidal dependence on θ
A	Constant in $\bar{W}_2$ in terms of body geometry
$\bar{V}_{n2}$	Non-dimensionalized velocity for case (1)
r_0	Body base length for unit axial length of body
σ_i	Body base angle
N	A constant defining a typical polygon case

Symbols

$\tan\delta_R$	Non-dimensionalized perpendicular distance from origin '0' to the inner body surface (σ_i = constant)
$\hat{m}$	Unit normal to the inner body surface
r_θ	Shock stand off distance from the origin
r_s	Shock stand off distance from the origin at $\theta = \pi/2 - \pi/N$
r_L	Shock stand off distance from the origin at $\theta = \pi/2$
$\hat{n}$	Unit normal to the shock
$\bar{n}$	Local normal to the shock
f	Magnitude of $\bar{n}$
$d\bar{s}$	Element surface area of the shock
$f_c(\sigma, M_\infty)$	Equivalent cone distribution
$(\bar{V}_n)_c$ =	$f_c(\sigma, M_\infty)$, equivalent cone distribution
$\phi(\sigma, M_\infty)$	Function related to f_c, $\phi = f_c/\tan\sigma$
θ^*	Constant [See Eq. 2.1]
$\tan\sigma_b^*$	A specific value of $\tan\sigma_b$ corresponding to $\theta = \theta^*$
θ_s	Semi angle of the equivalent cone, i.e. of equal base area to wave rider, see Eq. 1.9
M_∞	Free stream Mach number
a_∞	Free stream sonic velocity

Symbols

μ	Mach angle
C_p	Specific heat at constant pressure
C_v	Specific heat at constant volume
γ	Ratio of specific heats
ε	$= (\gamma-1)/(\gamma+1)$
T_0	Free stream stagnation temperature
a_0	Sonic velocity at stagnation temperature
$g(\sigma,\theta,M_\infty)$	Function to be determined from symmetry constraints in case (3)
$\vec{V}_1$	Velocity vector behind an oblique shock
V_1	Magnitude of velocity vector $\vec{V}_1$
$\hat{V}_1$	Unit velocity vector behind an oblique shock
T	Axis parallel to Z axis, Figure (1)
$\hat{t}$	Unit vector along T axis, see Eq. (1e)
v_t	Component of $\vec{V}_1$ along T axis, Figure (1)
v_x	Component of $\vec{V}_1$ along X axis, Figure (1)
ρ	Density
S	Entropy
P	Pressure
r_c	Equivalent cone shock stand off distance from the origin

Subscripts

$[\quad]_b$	Condition at the body
$[\quad]_s$	Condition at the shock
$[\quad]_d$	Design condition

CHAPTER I

INTRODUCTION

In 1959, G.I. MAIKAPAR (U.S.S.R) and T. NONWEILLER (England), suggested that by taking stream surfaces behind plane shock waves as rigid boundaries, a class of three dimensional bodies are formed.

For such a class of bodies the leading edges appear as the intersection between the plane shock and the stream surfaces.

The aerodynamic characteristic of these bodies are obtained on using plane shock relations at the given M_d termed as the design Mach number.

This essentially inverse approach has been applied for example to two shock configurations to obtain different geometries [1,2].

Also different classes of bodies, with curved inner boundaries have been obtained, using conical flow between two intersecting shocks obtained from cones at zero angle of attack [3].

Here the former case, (i.e. N-symmetric bodies with polygonal cross sections) are considered, with cross-sectional distributions that do not vary along the axial length (Figure (1)).

For departures of M_∞ from design Mach number (M_d), the shock is not planar.

Hence, due to the variation of shock strength, the flow is rotational. Depending on the departure of M_∞ from M_d, three marked shock configurations are obtained.

(1) $|M_\infty - M_d| << M_d$. The velocity distribution could be obtained by perturbing the design velocity components, hence the resulting shock could be taken as the perturbed planar shock.

(2) $M_\infty > M_d$. In this case, one would expect that the attached plane shock would move towards the body, with possible shock interactions and reflections from the inner boundary. This becomes clear if the flow is considered for a wedge in plane (R'), Figure (1) perpendicular to the leading edge OL.

(3) $M_\infty < M_d$. The shock is expected to move outwards away from the body, and depending on the magnitude $M_d - M_\infty$, it may either remain attached or detach from the leading edges.

The latter case has been considered here. But due to non-linearity of the field equation, the only possible solutions are those resulting from the use of numerical computations.

However, the approach here has been to take accurate numerical velocity distributions [4], of an equivalent cone,

(i.e. a cone with equal base area at the same M_∞) and modify them so as to accommodate the symmetry and tangency condition at the body.

Also, a relation between velocity components has been obtained at the outer boundary (shock), unknown a priori. This relation is then used to obtain the shock location for the given approximation.

However, with infinite choices of approximations, a corresponding infinite number of shock configurations could be obtained for a given geometry and M_∞.

The question then arises, which approximated distribution, if any, would be reasonable.

It is shown that with typical distributions satisfying the boundary conditions, some reasonable results are obtained. The best choice for such distributions, of course, requires that some comparison be made with experimental results.

CHAPTER 2

DESCRIPTIVE EQUATIONS

Point O (Figure (2)) is the origin of the spherical coordinate system r,σ,θ (angle measured positive from negative x,z axis), and also is the apex of the conical flow.

Since the flow is conical, it follows that

$$\frac{\partial(\text{flow properties})}{\partial r} = 0$$

Hence, the Eulerian equations in a spherical coordinate system become [5]

$$V_n \frac{\partial V_r}{\partial \sigma} + \frac{W}{\sin\sigma} \frac{\partial V_r}{\partial \theta} = V_n^2 + W^2$$

$$V_n \frac{\partial V_n}{\partial \sigma} + \frac{W}{\sin\sigma} \frac{\partial V_n}{\partial \theta} + \frac{1}{\rho} \frac{\partial P}{\partial \sigma} + V_r V_n - W^2 \cot\sigma = 0 \qquad (1)$$

$$V_n \frac{\partial W}{\partial \sigma} + \frac{W}{\sin\sigma} \frac{\partial W}{\partial \theta} + \frac{1}{\rho \sin\sigma} \frac{\partial P}{\partial \theta} + V_r W + V_n W \cot\sigma = 0$$

Here V_r and V_n are velocity components along and normal to a radius, r, respectively in the meridian plane θ = constant, and W is normal to this plane (Figure (2)).

Neglecting heat conduction and body forces and assuming constant total enthalpy, the adiabatic energy equation provides two additional relations. When solved

together with equations (1) and the continuity equation, the rotational field equation is obtained [5]

$$V_r\left(2 - \frac{V_n^2 + W^2}{a^2}\right) + V_n \cot\sigma + \frac{\partial V_n}{\partial \sigma}\left(1 - \frac{V_n^2}{a^2}\right) + \frac{1}{\sin\sigma}\frac{\partial W}{\partial \theta}\left(1 - \frac{W^2}{a^2}\right)$$

$$- \frac{WV_n}{a^2}\left(\frac{1}{\sin\sigma}\frac{\partial V_n}{\partial \theta} + \frac{\partial W}{\partial \sigma}\right) = 0 \qquad (1.1)$$

This is essentially a relation between velocity components throughout the conical field.

CHAPTER 3

BOUNDARY CONDITIONS (TANGENCY CONDITION AT THE BODY)

Now spherical velocity components V_r, V_n, W can be expressed in terms of a cartesian coordinate system XYZ with origin at 0 (Figure 2).

$$\vec{V}_r = -\hat{i}(V_r\cos\sigma) + \hat{j}(V_r\sin\sigma\cos\theta) - \hat{k}(V_r\sin\sigma\cos\theta)$$

$$\vec{V}_n = \hat{i}(V_n\sin\sigma) + \hat{j}(V_n\cos\sigma\sin\theta) - \hat{k}(V_n\cos\sigma\cos\theta) \qquad (1.2)$$

$$\vec{W} = \hat{j}(W\cos\theta) + \hat{k}(W\sin\theta)$$

The tangency condition at the body is given by $\hat{m}\cdot(\vec{V}_n + \vec{W}) = 0$, where $\hat{m}$ is a unit normal to the inner surface of a body. This last relation implies that (Appendix A):

$$\left(\frac{W}{V_n}\right)_b = \frac{\cot(\sigma_i-\theta)}{\cos\sigma_b} \qquad (1.3)$$

On the body $\sigma_b = \sigma_b(\theta)$ (Appendix A); hence $(W/V_n)_b$ is essentially a function of θ for a given geometry.

A number of $(W/V_n)_b$ distributions on the basis of the equation (1.3) are shown in Figures (3.a, 3.b), for different σ_i base angle, r_0 base lengths for bodies with unit axial lengths (i.e., r_0 is in units of axial length), and N = 4 as a typical polygon case.

3.1 Symmetry Conditions

From symmetry considerations, one must require the individual velocity component distributions to be such that

$$(W)_{\theta=\pi/4} = 0 \qquad (W)_{\theta=\pi/2} = 0 \qquad [(V_n)_b]_{\theta=\pi/4} = 0$$

$$[(V_n)_b]_{\theta=\pi/2} = 0 \tag{1.4}$$

and

$$(\frac{\partial V_n}{\partial \theta})_{\theta=\pi/4} = 0 \qquad (\frac{\partial V_n}{\partial \theta})_{\theta=\pi/2} = 0 \tag{1.5}$$

In particular, conditions (1.4 and 1.5) require V_n and W to be symmetric and antisymmetric about the $\theta = \pi/4, \pi/2$ dividing planes for the polygon section.

3.2 Entropy Considerations

The entropy distribution in the cross plane is given by (see [5]):

$$V_n \sin\sigma \frac{\partial S}{\partial \sigma} + W \frac{\partial S}{\partial \theta} = 0 \tag{1.6}$$

This implies that the variation of entropy is related to the velocity components and shows that the entropy may be indeterminate at certain points where W and V_n are both zero simultaneously. Therefore, a singular point of entropy

exists and hence all of the streamlines in the plane must converge to such a point or points.

The stronger shock in the region of $\theta = \pi/2$ implies a pressure field such that the streamlines are expected to converge to point E (Figure (4a); therefore, $W < 0$ and $V_n < 0$ throughout the field and

$$\left(\frac{\partial W}{\partial \theta}\right)_{\theta=\pi/2} < 0 \qquad \left(\frac{\partial W}{\partial \theta}\right) < 0 \tag{1.7}$$

CHAPTER 4

DISTRIBUTIONS RELATED TO THE EQUIVALENT CONE

Equating the base area of the wave rider (its geometry to be determined) to its equivalent cone (a cone with equal base area) gives:

$$\tan\sigma_i = \frac{\pi \tan^2\theta_s \tan\frac{\pi}{N}}{N r_0^2 \tan\frac{\pi}{N} - \pi \tan^2\theta_s} \tag{1.8}$$

where θ_s is the cone semi angle at the same M_∞ as the wave rider under consideration.

Now assume that $\overline{W}$ and $\overline{V}_n$ for a body of this class with geometry specifications σ_i, r_0 satisfying Equation (1.8) are related to the equivalent cone distribution, $(V_n)_c = f_c(\sigma, M_\infty)$. For that body, compatible $\overline{W}$ and $\overline{V}_n$ distributions will be shown to exist.

CHAPTER 5

APPROXIMATIONS AND ASSUMPTIONS

In relating the wave rider distributions to $f_c(\sigma, M_\infty)$, it is assumed that:

(1) The functional dependence of $\bar{W}$ on the θ and σ coordinates is separable.

(2) The dependence of $\bar{W}$ on σ and M_∞ is taken to be the same as its equivalent cone $f_c(\sigma, M_\infty)$, or a modified form of f_c.

(3) The dependence of $\bar{W}$ on θ has a sinusoidal behaviour as seen to be consistent with the boundary conditions.

(4) $\bar{V}_n$ is such that the ratio $(\bar{W}/\bar{V}_n)_b$ at the body takes on specific values given by the tangency conditions.

(5) Constants present in both $\bar{W}$ and $\bar{V}_n$ distributions could be obtained by satisfying the symmetry constraints.

(6) For N large, the distributions tend continuously to their equivalent cone values.

On the basis of the last two assumptions, the distributions are divided into three cases.

CHAPTER 6

CASES AND INTERPRETATION OF THE CASES

Case (1): Distributions satisfying no symmetry conditions.

Case (2): Distributions satisfying a partial symmetry constraint.

Case (3): Distributions satisfying all symmetry conditions.

Case (1)

A distribution of velocity components, for which $(\partial V_n/\partial\theta) \neq 0$ on symmetry lines, can be written as

$$\bar{W}_1 = C_0 \sin(\tfrac{\pi}{2}-\theta)\sin(\theta-\tfrac{\pi}{2}+\tfrac{\pi}{N})\sin(\theta-\sigma_i)\phi(\sigma,M_\infty)$$

$$\bar{V}_{n1} = \frac{\bar{W}_1 \cos\sigma_b}{\cot(\theta-\sigma_i)} + [\tan\sigma - \frac{C_0 r_0}{\sin\theta + \frac{\cos\theta}{\tan\sigma_i}}]\phi(\sigma,M_\infty) \tag{1.9}$$

The choice of these distributions is consistent with the assumptions discussed in Chapter 5.

On the body, $\sigma_b = \tan^{-1}[r_0/(\sin\theta + \cos\theta/\tan\sigma_i)]$ (see Appendix A). The constant C_0 is unity for the wave rider body segment under consideration and zero to correspond to a cone. That is, for an equivalent cone, $\bar{V}_n = (\bar{V}_n)_c = \tan\sigma\phi(\sigma,M_\infty)$, which is set equal to values obtained from cone tables [4] (i.e., $f_c(\sigma,M_\infty)$. Hence, $\phi(\sigma,M_\infty) = f_c/\tan\sigma$.

Of course, the approximate assumed dependence of $\bar{W}$ and $\bar{V}_n$ on θ could be varied. Though it is logical to assume that $\bar{W}$ varies sinusoidally with θ, another $\bar{W}$ approximation which does not exhibit this totally has been considered for comparison.

$$\bar{W}_2 = C_0(\theta-\tfrac{\pi}{2}+\tfrac{\pi}{N})^{1/3}\sin(\tfrac{\pi}{2}-\theta)\sin(\theta-\sigma_i)\tan\sigma\phi(\sigma,M_\infty)$$

$$\bar{V}_{n2} = \frac{\bar{W}_2\cos\sigma_b}{\cot(\theta-\sigma_i)} + [\tan\sigma - (C_0r_0/(\sin\theta + \cos\theta/\tan\sigma_i)]\phi(\sigma,M_\infty) + C_0[\tan\sigma - C_0r_0/(\sin\theta + \cos\theta/\tan\sigma_i]\phi \qquad (2)$$

Both approximations satisfy the boundary conditions of Case (1), but will clearly result in different shock shapes, and furnish some measure of the sensitivity of the results to specific distribution choices.

Case (2)

A distribution that satisfies $(\partial V_n/\partial\theta)_{\theta=\pi/2-\pi/N} = 0$ can be written as:

$$\bar{W} = \frac{-r_0\sin\sigma_i}{\sin(\frac{\pi}{N}+\sigma_i)\sin\frac{\pi}{N}(\cos\sigma_b)_{\theta=\pi/2-\pi/N}} \frac{\cos(\theta+\frac{\pi}{N})\cos\theta f_c}{|(\tan\sigma - \tan\sigma_b^*)|} \qquad (2.1)$$

where

$$A = \frac{-r_0\sin\sigma_i}{\sin(\frac{\pi}{N}+\sigma_i)\sin\frac{\pi}{N}(\cos\theta_b)_{\theta=\pi/2-\pi/N}}$$

and

$$\bar{V}_n = \frac{\bar{W}\cos\sigma_b}{\cot(\theta-\sigma_i)} + \frac{1}{|\tan\sigma - \tan\sigma_b^*|}\left[\tan\sigma - \frac{r_0\sin\sigma_i}{\cos(\theta-\sigma_i)}\right]f_c$$

Where the value of the constant, A, in $\bar{W}$ is written in terms of body geometry and is obtained in such a way that the partial symmetry constraint is satisfied. The body under consideration may be assumed to have an attached infinitely small thin plate in the plane $\theta = \pi/2$, so that the condition $(\partial V_n/\partial\theta)_{\theta=\pi/2} = 0$ is justified. Also, in Equation (2.1), $\cos\sigma_b = \tan^{-1}(r_i)$.

A suitable choice for $\tan\sigma_b^*$ and subsequently θ^* needs explanation: the tangent of σ_b^* is representative of the radial distance from the body to the origin. This radial distance is seen to tend to a constant length in the limit as $N \to \infty$.

This is necessary to ensure that as $N \to \infty$, $W \to 0$ and $V_n \to f_c(\sigma,M_\infty)ds$ in assumption (6) (see Chapter 5, Assumptions and Approximations). Hence, the "angle" θ^*, defining $\tan\sigma_b^*$, is an appropriate "mean" angle in the range of $\pi/2 - \pi/N \leq \theta \leq \pi/2$.

Since $\pi/2 - \pi/N \leq \theta \leq \pi/2$ as $N \to \infty$, $\theta \to \pi/2$, that is to say, the range of θ under consideration becomes very small and tends to $\pi/2$.

It is justified for large N, to write $\theta \simeq \theta^* \to \pi/2$, i.e. $\tan\sigma_b = r_0 \sin\sigma_i / \cos(\theta-\sigma_i) \to r_0$ and $\tan\sigma_b^* \to r_0$. That is, for large N, the body tends to a saw tooth cone, with average radius r_0.

For that cone, from Equation (2.1)

$$\bar{W} = \left[\frac{r_0 \cos\theta f_c}{(\cos\sigma_b)\,|\tan\sigma - r_0|}\right]^{\theta\to\pi/2}$$

Hence, away from the rough surface of this cone (σ, increasing), for $\tan\sigma > r_0$, $\bar{W}$ tends to zero.

For $\tan\sigma = r_0$, at the surface of the saw tooth cone, there is a singularity for $\bar{W}$. Hence, a boundary_layer type of problem occurs locally at the surface.

Also, from Equation (2.1)

$$\bar{V}_n \to 0\cdot(\bar{W}) + \frac{\tan\sigma - \tan\sigma_b}{|\tan\sigma - \tan\sigma_b^*|} f_c \qquad (2.2)$$

Previous arguments showed that for $N \to \infty$, $\tan\sigma_b$, and in particular, $\tan\sigma_b^* \to r_0$. From Equation (2.2), $\bar{V}_n \to 0\cdot(\bar{W}) + f_c$, so away from the body, $\bar{V}_n \to f_c(\sigma, M_\infty)$ and assumption (6) is satisfied.

Naturally $\tan\sigma_b^*$ is varied by different choices of θ^*, from $\tan\sigma_b^* = r_i$ to $\tan\sigma_b^* = r_0$. The best choice of the "mean" angle θ^* is not possible, without analytical results available for comparison.

Case (3)

This case requires $(\partial V_n/\partial\theta) = 0$ on both symmetry lines which essentially represents a wave rider without an attached plate.

A distribution for $\bar{W}$ and $\bar{V}_n$ could be written as:

$$\bar{W} = \frac{\cos\theta\cos(\theta+\frac{\pi}{N})\, g(\sigma,\theta,M_\infty)}{|\tan\sigma-\tan\sigma_b^*|} \tag{2.3}$$

$$\bar{V}_n = \frac{\bar{W}\cos\sigma_b}{\cot(\theta-\sigma_i)} + \frac{1}{|\tan\sigma-\tan\sigma_b^*|}\left[\tan\sigma - \frac{r_0\sin\sigma_i}{\cos(\theta-\sigma_i)}\right] f_c$$

However, this does introduce an inconsistency; that is, it will not satisfy $\bar{W} < 0$ throughout the field required by the entropy distribution that all the streamlines convege to point E, Figure (4a).

If the streamlines in the neighborhood of $\theta = \pi/2-\pi/N$ are assumed to converge to point E, so that $(\partial\bar{W}/\partial\theta) < 0$, and streamlines near $\theta = \pi/2$ are assumed to converge to point B, Figure (4a), then the requirement of $(\partial V_n/\partial\theta) = 0$, on both symmetry lines will imply:

$$g(\sigma,\theta,M_\infty) = \frac{-r_0\sin\sigma_i f_c}{\sin(2\theta+\frac{\pi}{N})\cos\sigma_b\cos(\theta-\sigma_i)} \tag{2.4}$$

This avoids the inconsistency, but introduces instead a singularity for $\bar{W}$ and $\bar{V}_n$ at $\theta = \pi/2 - \pi/2N$, which unfor-

tunately is no better than the inconsistency.

It can be shown that this singularity is removed by assuming that the distribution is discontinuous at $\theta = \pi/2 - \pi/2N$. However, the physical meaning is then quite unclear, though all the boundary conditions and symmetry constraints are then satisfied.

CHAPTER 7

BOUNDARY CONDITIONS AT THE CONICAL SHOCK

For a general three dimensional shock, one could use the oblique shock relations (for a plane flow), as long as the velocity components and Mach number post and pre-shock are projected along $\hat{n}$, the unit local normal to the shock, Appendix (C). Hence from plane shock relations, one obtains:

$$\frac{\vec{U}_\infty \cdot \vec{n}}{(\vec{V}_n + \vec{W}) \cdot \vec{n}} = \frac{(\gamma+1)(M_\infty \cdot \hat{n})^2}{2 + (\gamma-1)(M_\infty \cdot \hat{n})^2} \tag{2.5}$$

where $\hat{n}$, in particular for a conical shock is given by Appendix (C), and $\vec{V}_n$ and $\vec{W}$ are given by Equation (1.2) and $(V_r)_s = -U_\infty \cos\sigma_s$

$$\hat{n} \cdot \vec{U}_\infty = \frac{-(V_n + U_\infty \sin\sigma)\sin\sigma}{[W^2 + (V_n + U_\infty \sin\sigma)^2]^{1/2}}$$

$\hat{n} \cdot (\vec{V}_n + \vec{W})$, after expansion, is reduced to (2.6)

$$\hat{n} \cdot (\vec{V}_n + \vec{W}) = \frac{W^2 + V_n(V_n + U_\infty \sin\sigma)}{[W^2 + (V_n + U_\infty \sin\sigma)]}$$

$$M_\infty \cdot \hat{n} = \frac{-M_\infty (V_n + U_\infty \sin\sigma)\sin\sigma}{[W^2 + (V_n + U_\infty \sin\sigma)^2]^{1/2}}$$

Throughout this section, the subscript $[\,]_s$ has been omitted for simplicity knowing that all the relations hold

only at the shock.

Substituting Equation (2.6) into Equation (2.5):

$$-(\gamma+1)M_\infty^2\sin\sigma[V_n(V_n+U_\infty\sin\sigma)+W^2][V_n+U_\infty\sin\sigma]$$

$$= U_\infty[2W^2+2(V_n+U_\infty\sin\sigma)+(\gamma-1)M_\infty^2\sin^2\sigma(V_n+U_\infty\sin\sigma)^2]$$

Non dimensionalizing the last equation with respect to

$$V_n' = V_n/U_\infty \qquad W' = W/U_\infty \qquad V_r' = V_r/U_\infty$$

the above relation becomes:

$$-(\gamma+1)M_\infty^2\sin\sigma[V_n'(V_n'+\sin\sigma)+W'^2][V_n'+\sin\sigma]$$

$$= [2W'^2+(V_n'+\sin\sigma)^2(2+(\gamma-1)M_\infty^2\sin^2\sigma)] \qquad (2.7)$$

and also $V_r' = \cos\sigma$

Hence, behind a conical shock, two relations between velocity components V_n', V_r', W' exist. Again, relations (2.7) apply as well to a right circular shock (obtained from a cone at zero angle of attack). For the cone, $W' = 0$ Equation (2.7) reduces to

$$-(\gamma+1)M_\infty^2\sin^2\sigma V_n' = 2+(\gamma-1)M_\infty^2\sin^2\sigma$$

which is the expected simplified shock relation.

CHAPTER 8

STEP BY STEP CALCULATIONS

Once the distributions $\bar{W}$ and $\bar{V}_n$, related to $f_c(\sigma, M_\infty)$, are evaluated based on the assumptions made, the shock condition may be used to determine the shock location in each case.

For constant θ, and with $\sigma_b \leq \sigma \leq \sigma_s$, for each increment of angle "σ", the numerical evaluations of $\bar{W}$ and $\bar{V}_n$ is possible using the corresponding $f_c(\sigma, M_\infty)$ from Kopal tables.

With the angle "θ" kept constant, a numerical evaluation for specific $\bar{W}$ and $\bar{V}_n$ values from Equation (2.7) yields that $\sigma = \sigma_s$ that corresponds to a shock location. That is, wherever the numerical values of $\bar{W}$ and $\bar{V}_n$ satisfy the shock relation a corresponding shock location is possible.

Once the shock shapes are determined in each case, the results may be examined on physical grounds for consistency.

CHAPTER 9

DISCUSSION OF NUMERICAL RESULTS

The results obtained were limited to the configuration N = 4. The relations could equally well be applied to other values of N.

For the case $(\partial V_n/\partial\theta) \neq 0$ on both symmetry lines: the shock shapes for various distributions are shown on a normalized scale (r/r_s versus θ), where r_s is the shock stand off distance at $\theta = \pi/2 - \pi/2N$ from the origin, 0.

Table (3) shows a tabulation of M_∞, σ_i, r_0, r_L/r_s (where r_L is shock stand off distance at $\theta = \pi/2$), and r_i is relative unit length axially, with the equivalent cone semi angle $\theta_s = 20°$.

Figure (6) shows the polar plot of shock shapes at a constant $M_\infty = 1.6054$ for different bodies with distributions $\bar{W}_2$, $\bar{V}_{n2}$ (see Equation (2)). Both results show sharp variations in shock shape (Table (3)), which do not appear to be reasonable on physical grounds.

However, Figure (6) shows the shock distribution for the smallest considered $M_\infty = 1.6054$, which corresponds essentially to being near detachment for the equivalent cone [4].

Therefore, as the flow for the body was related to the cone, one would perhaps expect to encounter difficulties at the smaller M_∞.

Hence, other values of M_∞ were tried, for $M_\infty = 1.8714$ and $\sigma_i = 45°$.

Figure (7) again indicates shocks with sharp variations [see (r_L/r_s), from Table (3)], which still do not seem reasonable on physical grounds.

Essentially, the distributions that did not satisfy $(\partial V_n/\partial\theta) = 0$ did not give reasonable results.

For the case $(\partial V_n/\partial\theta)_{\theta=\pi/2-\pi/N} = 0$ and cone semi angle $\theta_s = 20°$ and $\theta^* = 65°$, the shock shapes are shown in Figure (8) on the same normalized scale. The results accompanied by Table (4) appear consistent. That is, as M_∞ increases, the shock is seen to move towards the body. Also the shock stand off distance variation is smooth, and finally, the shock strength at $\theta = \pi/2$ is stronger than at $\theta = \pi/4$, as expected.

However, for $M_\infty = 1.6054$, the shock shape is seen to have a sharp discontinuity in the neighborhood of $\theta = \pi/2$. This is again believed to be due to the near detachment condition for the equivalent cone.

To show this, a small change in $M_\infty = 1.6531$ was considered (Figure (8)). The shock shape is seen to be consistent. Figure (9) shows shock shapes for different bodies at

at $M_\infty = 1.8714$ with $\theta_s = 20°$, $\theta^* = 65°$. The results are again seen to be reasonable.

Figure (10) shows the same shock shapes on a normalized scale (r/r_c versus θ), where r_c is the shock radius of the equivalent cone at $M_\infty = 1.8714$.

Figure (10) also shows that for both $\sigma_i = 22.12°$ and $\sigma_i = 45°$ (at $\theta = 45°$), the shocks are inside the equivalent conical shock, but for $\sigma_i = 61.7°$, it lies outside. This is as expected physically in view of the shape of the bodies considered.

The results for the case $(\partial V_n/\partial\theta) = 0$ were for $\theta_s = 20°$ (equivalent cone, semi angle). Since the relative size of the disturbed region is related to the particular M_∞, θ_s combination, a $\theta_s = 30°$ case was also completed [Figure (11) with the corresponding Table (5)].

A comparison between r_L from Tables (4) and (5) shows that for $\theta_s = 30°$, the shocks move away from the body for the same σ_i. This is reasonable, of course, since for a given σ_i, increasing θ_s increases r_0.

The choice of $\theta^* = 65°$ was based on the reasonableness of results. An indication of the sensitivity of the distribution to θ^* follows from the $\theta^* = 73°$ results for $M_\infty = 2.13$, and 1.87, 1.65 (all for $\sigma_i = 22.12°$) as shown

in Figure (12). The change from 65° to 73° has an appreciable effect on shock shape (Figure (12) and Table (6)) and leads, in fact, to unrealistic contours.

CHAPTER 10

CONCLUSION

An analytical approach to deriving shock shapes for different bodies with polygonal cross-sections seems to fail for Case (1), i.e. $(\partial V_n/\partial\theta) \neq 0$ on both symmetry lines.

This is essentially attributed to the failure in satisfying the necessary boundary condition $(\partial V_n/\partial\theta) = 0$, as was expected, but provides a measure of the symmetry condition importance. More importantly, there was no information provided in the corresponding distributions $(\bar{W}_1, \bar{W}_2)$ and $(\bar{V}_{n1}, \bar{V}_{n2})$ about the fact that as $N \to \infty$, the velocity distributions should, in fact, approach their equivalent cone values continuously.

For the case of $(\partial V_n/\partial\theta) = 0$ with a plate attached to the body at $\theta = \pi/2$, reasonable results were obtained.

It was mentioned that there could be other discrete (or a range of) values of θ^*, which might give equally reasonable results. However, without experiments, to make comparison with, a best choice of θ^* is not possible at this time.

One distribution has been suggested for the case of $(\partial V_n/\partial\theta) = 0$ on both symmetry lines. As mentioned before,

this makes use of the implied assumption that the component of the velocity field is discontinuous at some intermediate value of θ.

Interesting as it is, physically it is impossible for $\bar{W}$ to be discontinuous at some θ in the flow field.

Finally, for part (2), i.e. $M_\infty > M_d$ [See Introduction] a form of $\bar{W}$ and $\bar{V}_n$ could be written as:

$$\bar{W} = \bar{W}_d + \xi(M_\infty, M_d, \sigma, \theta)$$

$$\bar{V}_n = \bar{V}_{nd} + \Psi(M_\infty, M_d, \sigma, \theta)$$

where $\bar{W}_d$ and $\bar{V}_{nd}$ are the velocity components at the design condition obtained in Appendix (E).

The choice of ξ or Ψ should be such that at $M_\infty = M_d$ $\xi = \Psi = 0$. This would give results for a caret wing with attached shock at off design condition. The necessary boundary conditions are $(\partial V_n/\partial\theta)_{\theta=\pi/4} = 0$ and $(\partial V_n/\partial\theta)_{\theta=\pi/2} \neq 0$.

Once distributions for $\bar{W}$ and $\bar{V}_n$ are selected, in principle, one can find $\bar{V}_r$ throughout the whole flow field [Appendix (d)].

Overall, the approach to obtain consistent results from satisfying boundary conditions with typical distributions is reasonable in case (2) (partial symmetry condition). However, it leads to physically meaningless results in Case

(1) (no symmetry constraints).

The approach is clearly time saving in comparison to numerical computation of the field equation. Hence, in Case (2), quick reasonable results could be obtained as a guide to the shock shapes found from experiment.

As the wave rider velocity distributions are related to the equivalent cone, for higher M_∞ the approximations may not be reliable. This is due to the fact that for higher M_∞, the cone shock will move closer to the surface of the cone. Hence, this limits the range of the cone field "σ". This, in turn, leads to long range extrapolations for obtaining results for the wave rider.

Care should also be taken for smaller M_∞, where the cone shock would be near detachment.

At a given M_∞, the approximations should be reliable for different aspects ratio bodies, r_0. As long as this does not vary θ_s (equivalent cone semi angle) to encounter the two preceding situations discussed above.

APPENDIX A

OBTAINING THE INNER BOUNDARY CONDITION

From Figure (2b), taking the origin of the Cartesian coordinate system at O, hence:

$$\overline{OB} = +r_0\hat{j} - \hat{i}$$

and

$$\overline{OE} = |OE|(\cos\tfrac{\pi}{N}\hat{j} - \sin\tfrac{\pi}{N}\hat{k})$$

But from Figure (4a) $|OE| = \tan\delta$, and also

$$\frac{\sin\sigma_i}{\tan\delta} = \frac{\sin(\sigma_i+\pi/N)}{r_0}$$

Hence, $\overline{OE} = \tan\delta(\cos\tfrac{\pi}{N}\hat{j} - \sin\tfrac{\pi}{N}\hat{k})$

where

$$\delta = \tan^{-1}(r_0\sin\sigma_i/\sin(\sigma_i-\pi/N)$$

The unit normal $\hat{m}$ to the body, i.e. the plane OEL from Figure (1) could be written as

$$\hat{m} = \alpha\hat{i} + \beta\hat{j} + \gamma\hat{k} \qquad (1.a)$$

but $\hat{m}\cdot\overline{OC} = 0$ and also $\alpha^2 + \beta^2 + \gamma^2 = 1.$

These three equations will determine α, β, γ, hence

$$\hat{m} = \hat{i}\sin\delta_R + \sin\sigma_i\cos\delta_R\hat{j} - \cos\sigma_i\cos\delta_R\hat{k} \qquad (2.a)$$

where

$$\delta_R = \tan^{-1}(r_0\sin\sigma_i) = \tan^{-1}(\sin(\sigma_i+\pi/N)\tan\delta)$$

But, by the tangency condition at the body:

$$[\hat{m}\cdot(\vec{V}_n + \vec{W}]_b = 0$$

as $\vec{V}_r$ has no component along $\hat{m}$.

Where $\hat{m}$, $\vec{V}_n$, $\vec{W}$ are given respectively by Equations (2.a) and (1.2), $\hat{m}\cdot(\vec{V}_n + \vec{W})$ could be written as:

$$[\hat{m}\cdot(\vec{V}_n + \vec{W})]_b = (\sin\delta_R\sin\sigma_b)V_n + \cos\delta_R[\sin\sigma_i(\cos\sigma_b\cos\theta V_n + W\cos\theta) - \cos\sigma_i(-V_n\cos\sigma_b\cos\theta + W\sin\theta)] = 0$$

From which corresponds:

$$(W/V_n)_b = \frac{\tan\delta_R\sin\sigma_b + \cos\sigma_b\cos(\theta-\sigma_i)}{\sin(\theta-\sigma_i)} \qquad (3.a)$$

But at the body also $\hat{m}\cdot\vec{V}_r = 0$ where $\vec{V}_r$ is given by Equation (1.2)

$$\hat{m}\cdot\vec{V}_r = -V_r\cos\delta_R[\cos\sigma_b\tan\delta_R - \sin\delta\cos(\theta-\sigma_i)] = 0$$

implying

$$\tan\delta = \tan\sigma_b\cos(\theta-\sigma_i)$$

Substituting for $\tan\delta_R$ in Equation (3.a)

$$(W/V_n)_b = \cot(\sigma_i-\theta)/\cos\sigma_b \qquad (4.a)$$

However from Figure (4a) it could be shown that:

$$\sigma_b = \tan^{-1}(r_0\sin\sigma_i/\cos(\sigma_i-\theta)) \qquad (5.a)$$

so that

$$(W/V_n)_b = \chi(\sigma_i,\sigma(\theta))$$

APPENDIX B

ALTERNATIVE WAY OF OBTAINING INNER BOUNDARY CONDITION FROM ENTROPY CONSIDERATIONS

The entroy distribution in an isentropic flow is given by Equation (1.6) as:

$$V_n \sin\sigma (\partial S/\partial\sigma) + W(\partial S/\partial\theta) = 0 \qquad (1.b)$$

and since the flow is isentropic

$$(d\bar{\ell}\cdot\nabla)S = 0$$

where $d\bar{\ell}$ is an increment along a stream line.

This implies

$$\frac{\partial S}{\partial\sigma}\frac{\partial\sigma}{\partial\ell} + \frac{\partial S}{\partial\theta}\frac{\partial\theta}{\partial\ell} = 0$$

Comparing Equation (1.b) with the above relation:

$$(W/V_n)_b = (d\theta/d\sigma)_\sigma \sin\sigma \qquad (2.b)$$

This relation is true along any stream line, or on any stream lines surface, one of which is the inner boundary of the body.

From Appendix (A), Equation (5.a)

$$\sigma_b = \tan^{-1}(r_0 \sin\sigma_i / \cos(\sigma_i - \theta))$$

implying

$$(d\theta/d\sigma)_b = \frac{(\sin\theta + (\cos\theta/\tan\sigma_i)^2 + r_0^2}{r_0(\cos\theta - \sin\theta(1/\tan\sigma_i)}$$

Substituting for $(d\theta/d\sigma)_b$ in Equation (2.b), it can be shown that

$$(W/V_n)_b = \cot(\sigma_i - \theta)/\cos\sigma_b \qquad (3.b)$$

Which is exactly the relation obtained in [Appendix (A)], using the tangency constraint.

APPENDIX C

DERIVING THE LOCAL NORMAL TO THE SHOCK IN TERMS OF THE VELOCITY COMPONENT

Figure (5) shows a three dimensional view of a conical shock surface R, on the assumption that the flow is conical, i.e. when V_r lies in the surface R.

The continuity equation in a plane tangent to an element of surface $d\bar{s}$ could be written as:

$$\vec{U}_\infty - (\hat{n}\cdot\vec{U}_\infty)\hat{n} = \vec{V}_r + \{\vec{V}_r + \vec{W} - [(\vec{V}_n + \vec{W})\cdot\hat{n}]\hat{n}\} \qquad (1.c)$$

where $\vec{U}_\infty$ is the uniform upstream velocity in the negative direction of the X axis, i.e.

$$\vec{U}_\infty = -U_\infty \hat{i} \qquad (2.c)$$

$$\hat{n} = \alpha\hat{i} + \beta\hat{j} + \gamma\hat{k}$$

where $\hat{n}$ is a unit normal to the element of surface ds positive outwards, written in Equation (2.c) in Cartesian coordinates. Hence from Equation (1.c), $\hat{n}$ is obtained in terms of velocity components. (In this section, the subscript $[\ ]_s$ is omitted for clarity, since all calculations are at the shock.) Substituting for U_∞ and $\hat{n}$ in Equation (1.c) gives

$$\text{L.H.S. Equation (2.c)} = \hat{i}(\alpha^2 U_\infty - U_\infty) + \hat{j}\alpha\beta U_\infty + \hat{k}\alpha\gamma U_\infty$$

$$\text{R.H.S. Equation (3.c)} = \hat{i}(V_n\sin\sigma - V_r\cos\sigma) + \hat{j}(V_n\cos\sigma\sin\theta + W\cos\theta + V_r\sin\sigma\sin\theta) + \hat{k}(W\sin\theta - V_r\sin\sigma\cos\theta - V_n\cos\sigma\cos\theta) - (\alpha\hat{i} + \beta\hat{j} + \gamma\hat{k})[\alpha V_n\sin\sigma + \beta(V_n\cos\sigma\sin\theta + W\cos\theta) + \gamma(W\sin\theta - V_n\cos\sigma\cos\theta)] \quad (3.c)$$

The R.H.S. of Equation (3.c) was obtained after substituting for $\hat{n}$, $\vec{V}_n$, and $\vec{W}$ from Equations (2.c) and (1.2) respectively in Equation (1.c).

Since the two vectors given by Equation (3.c) must be of the same magnitude and direction, hence a comparison of the two vectors gives: (in the ith direction)

$$(V_n\sin\sigma - V_r\cos\sigma) - \alpha^2 V_n\sin\sigma - \alpha\beta(V_n\cos\sigma\sin\theta + W\cos\theta) - \alpha\gamma(W\sin\theta - V_n\cos\sigma\cos\theta) = \alpha^2 U_\infty - U_\infty \quad (4.c)$$

(in the jth direction)

$$V_n\cos\sigma\sin\theta + W\cos\theta + V_r\sin\sigma\sin\theta - \alpha\beta V_n\sin\sigma - \beta^2(V_n\cos\sigma\sin\theta + W\cos\theta) - \beta\gamma(W\sin\theta - V_n\cos\sigma\cos\theta) = \alpha\beta U_\infty \quad (5.c)$$

(in the kth direction)

$$W\sin\theta - V_r\sin\sigma\cos\theta - V_n\cos\sigma\cos\theta - \alpha\gamma V_n\sin\sigma - \alpha\beta(V_n\cos\sigma\sin\theta + W\cos\theta) - \gamma^2(W\sin\theta - V_n\cos\sigma\cos\theta) = \alpha\gamma U_\infty \quad (6.c)$$

From these last three equations, the components α, β, γ in

Equation (2.c) are obtained as:

$\beta \times$ Equation (4.c) $- \alpha \times$ Equation (5.c) $\rightarrow$

$$\beta = \frac{\alpha(V_n \cos\sigma \sin\theta + W\cos\theta + V_r \sin\sigma \sin\theta)}{(V_n \sin\sigma - V_r \cos\sigma + U_\infty)} \qquad (7.c)$$

$\gamma \times$ Equation (4.c) $- \alpha \times$ Equation (5.c) $\rightarrow$

$$\gamma = \frac{\alpha(W\sin\theta - V_r \sin\sigma\cos\theta - V_n \cos\sigma\cos\theta)}{(V_n \sin\sigma - V_r \cos\sigma + U_\infty)}$$

Since $\hat{n}$ is a unit normal

$$\alpha^2 + \beta^2 + \gamma^2 = 1 \qquad (8.c)$$

Substituting for γ, β from Equation (7.c) in Equation (8.c):

$$\alpha = \frac{V_n \sin\sigma - V_r \cos\sigma + U_\infty}{f(V_r, V_n, W)}$$

where $f(V_r, V_n, W) = [(V_n \sin\sigma - V_r \cos\sigma + U_\infty)^2 + (V_n \cos\sigma \sin\theta + W\cos\theta + V_r \sin\sigma \sin\theta)^2 + (W\sin\theta - V_r \sin\sigma\cos\theta - V_n \cos\sigma\cos\theta)^2]^{1/2} \qquad (9.c)$

Substituting for α in Equation (7.c)

$$\beta = \frac{V_n \cos\sigma \sin\theta + W\cos\theta + V_r \sin\sigma \sin\theta}{f(V_r, V_n, W)}$$

$$\gamma = \frac{W\sin\theta - V_n\sin\sigma\cos\theta - V_r\cos\sigma\cos\theta}{f(V_r, V_n, W)}$$

Therefore, from Equation (2.c), $\hat{n}$ is obtained:

$$\hat{n} = \frac{1}{f}[(V_n\sin\sigma - V_r\cos\sigma + U_\infty)^2\hat{i} + (V_n\cos\sigma\sin\theta + W\cos\theta + V_r\sin\sigma\sin\theta)\hat{j} + (W\sin\theta - V_r\sin\sigma\cos\theta - V_n\cos\sigma\cos\theta)\hat{k}] \quad (10.c)$$

For a conical shock $(V_r)_s = U_\infty\cos\sigma_s$, hence substituting for V_r in Equation (9.c), $f(V_n, V_r, W)$ could be simplified:

$$f^2 = (V_n\sin\sigma - U_\infty\cos^2\sigma + U_\infty)^2\hat{i} + (V_n\cos\sigma\sin\theta + W\cos\theta + U_\infty\sin\sigma\cos\sigma\sin\theta)^2 + (W\sin\theta - U_\infty\cos\sigma\sin\sigma\cos\theta - V_n\cos\sigma\cos\theta)^2$$

expanded, f^2 could be reduced to

$$f^2 = W^2 + [V_n^2 + U_\infty\sin\sigma]^2$$

Substituting for f in Equation (10.c) and noticing that at the shock $(V_r)_s = (U_\infty\cos\sigma)_s$

$$\hat{n} = \frac{1}{[W^2 + (V_r + U_\infty\sin\sigma)^2]^{1/2}}\{[(V_n + U_\infty\sin\sigma)\sin\sigma]\hat{i} + [(V_n + U_\infty\sin\sigma)\cos\sigma\sin\theta + W\cos\theta]\hat{j} + [W\sin\theta - (V_n + U_\infty\sin\sigma)\cos\sigma\cos\theta]\hat{k}\} \quad (11.c)$$

If this $\hat{n}$ is valid for any conical shock surface, in particular, it should apply for a right circular shock. For a cone W = 0, Equation (11.c) reduces to:

$$\hat{n} = \hat{i}\sin\sigma + \hat{j}\cos\sigma\sin\theta - \hat{k}\cos\sigma\cos\theta$$

A comparison of this last equation with Equation (1.2) for $\vec{V}_n$ shows that $\hat{n}$ is then a unit normal in the $\vec{V}_n$ direction, which is the case corresponding to a cone at zero angle of attack.

Equation (11.c) applies to any conical shock surface, for which $\hat{n}$ is continuous, whereas Equation (10.c) furnishes the local normal for any shock, since Equation (10.c) was obtained without the use of the constraint that $(V_r)_s = U_\infty \cos\sigma_s$. Therefore, Equation (11.c) or (10.c) provides a functional form of $\hat{n}$, i.e.

$$\hat{n} = F(V_r, V_n, W)$$

APPENDIX D

REARRANGEMENT OF ROTATIONAL CONICAL FLOW EQUATIONS IN TERMS OF V_r

The rotational conical flow field equation in spherical coordinate system was stated as:

$$V_r[2a^2 - (V_n^2 + W^2)] + a^2 V_n \cot\sigma + a^2 \frac{\partial V_n}{\partial \sigma} - \frac{V_n}{2} \frac{\partial V_n^2}{\partial \sigma}$$
$$+ \frac{a^2}{\sin\sigma} \frac{\partial W}{\partial \theta} - \frac{W}{2} \frac{\partial W^2}{\partial \theta} - \frac{W}{2\sin\sigma} \frac{\partial V_n^2}{\partial \theta} - \frac{V_n}{2} \frac{\partial W^2}{\partial \sigma} = 0 \qquad (1.d)$$

But from the adiabatic energy equation:

$$a^2 = \left[\frac{2a_0^2}{\gamma-1} - (V_n^2 + V_r^2 + W^2) \right] \frac{\gamma-1}{2}$$

Substituting for a^2 in Equation (1.d) and rearranging some terms:

$$V_r \sin\sigma \{2a_0^2 - (V_n^2 + W^2)\gamma - (\gamma-1)V_r^2\} + \left[a_0^2 - \frac{\gamma-1}{2}(V_n^2 + W^2)\right.$$
$$\left. - \frac{\gamma-1}{2}V_r^2\right] \frac{\partial}{\partial \sigma}(V_n \sin\sigma) - \frac{V_n \sin\sigma}{2} \frac{\partial}{\partial \sigma}(V_n^2 + W^2) - \frac{W}{2} \frac{\partial}{\partial \theta}(V_n^2 + W^2)$$
$$+ \left[a_0^2 - \frac{\gamma-1}{2}V_r^2 - \frac{\gamma-1}{2}(V_n^2 + W^2)\right] \frac{\partial W}{\partial \theta} = 0$$

Expanding the above equation and factorizing a polynomial in terms of V_r, we obtain:

$$V_r^3(\gamma-1)\sin\sigma + \frac{V_r^2}{2}(\gamma-1)\left[\frac{\partial}{\partial\sigma}(V_n\sin\sigma) + \frac{\partial W}{\partial\theta}\right]$$

$$+ V_r[\gamma(V_n^2 + W^2)\sin\sigma + 2a_0^2\sin\sigma]$$

$$= a_0^2\frac{\partial}{\partial\sigma}(V_n\sin\sigma) - \left(\frac{\gamma-1}{2}\right)(V_n^2 + W^2)\left[\frac{\partial}{\partial\sigma}(V_n\sin\sigma) + \frac{\partial W}{\partial\theta}\right]$$

$$+ a_0^2\frac{\partial W}{\partial\theta} - \frac{V_n\sin\sigma}{2}\frac{\partial}{\partial\sigma}(V_n^2 + W^2) - \frac{W}{2}\frac{\partial}{\partial\theta}(V_n^2 + W^2) \qquad (2.d)$$

Hence, from Equation (2.d) $V_r = V_r(V_n, W, a_0(M_\infty))$ in the flow field.

APPENDIX E

OBTAINING W, V_n IN DESIGN CONDITIONS

In design condition stream lines are all parallel to the inner ridge line OE (Figure (1)). And all velocity field behind the oblique shock in the 'plane', say WGS, is given by:

$$\vec{V}_1 = \hat{i}v_x + \hat{t}v_t \tag{1.e}$$

i.e., where $\hat{t}$ is a unit vector along GT axis and v_x, v_t are corresponding components of $\vec{V}_1$ along axes X and T (Figure (1)), written in terms of U_∞:

$$\begin{aligned} v_x &= -U_\infty[1 - (1-\varepsilon)(\sin^2\sigma_s - \sin^2\mu)] \\ v_t &= -U_\infty\cot\sigma_s[(1-\varepsilon)(\sin^2\sigma_s - \sin^2\mu)] \end{aligned} \tag{2.e}$$

where $\sin\mu = a_\infty/U_\infty$ and $\varepsilon = (\gamma-1)/(\gamma+1)$.

Substituting in Equation (1.e) for v_x and v_t:

$$\vec{V}_1 = -U_\infty[1 - (1-\varepsilon)(\sin^2\sigma_s - \sin^2\mu)]\hat{i} - U_\infty\cot\sigma_s[(1-\varepsilon)(\sin^2\sigma_s - \sin^2\mu)]$$

Also, $\hat{t} = -\hat{j}\cos\frac{\pi}{N} + \hat{k}\sin\frac{\pi}{N}$ from Figure (4).

Hence, $\vec{V}_1$, in terms of XYZ coordinates, becomes:

$$\vec{V}_1 = -U_\infty[1 - (1-\varepsilon)(\sin^2\sigma_s - \sin^2\mu)]\hat{i} + U_\infty\cot\sigma_s[(1-\varepsilon)(\sin^2\sigma_s - \sin^2\mu)](\cos\tfrac{\pi}{N}\hat{j} - \hat{k}\sin\tfrac{\pi}{N}) \tag{3.e}$$

Also, if $\hat{V}_1$ is a unit vector along $\vec{V}_1$, then

$$\hat{V}_1 = -\hat{i}\cos\delta + \hat{j}\sin\delta\sin\frac{\pi}{N} - \hat{k}\sin\delta\cos\frac{\pi}{N} \qquad (4.e)$$

The spherical velocity components can now be expressed in terms of $\hat{V}_1$ since $V_n = V_1(\hat{V}_1\cdot\hat{V}_n)$, where $\hat{V}_n$ is a unit vector in the direction of $\vec{V}_n$ given by Equation (1.2). Substituting for $\hat{V}_1$, $\hat{V}_n$ in the above relation:

$$V_n = |\vec{V}_1\cdot\vec{V}_1|^{1/2}[-\sin\sigma\cos\delta + \sin\delta\cos\sigma\sin(\theta + \tfrac{\pi}{N})] \qquad (5.e)$$

Similarly

$$W = V_1\cdot(\hat{V}_1\cdot\hat{W}) \qquad \text{or} \quad W = |\vec{V}_1\cdot\vec{V}_1|^{1/2} \times [\cos(\theta + \tfrac{\pi}{N})]\sin\delta$$

and

$$V_r = V_1\cdot(\hat{V}_1\cdot\hat{V}_r) \qquad \text{or} \quad V_r = |\vec{V}_1\cdot\vec{V}_1|^{1/2}[\cos\delta\cos\sigma + \sin\delta\sin\sigma\sin(\theta + \tfrac{\pi}{N})]$$

where $|\vec{V}_1\cdot\vec{V}_1|^{1/2}$ is the magnitude of $\vec{V}_1$ given by Equation (3.e). Since the inner boundary condition is Mach number independent, hence

$$[W/V_N]_d = \frac{\cos(\theta + \pi/N)}{-\tan\delta\sin\sigma + \cos\sigma\sin(\theta + \pi/N)} \qquad (6.e)$$

must reduce to $(W/V_N)_b$ at off design conditions (Appendix (A)). From Equation (5.a) [Appendix (A)]:

$$\tan\delta = [\tan\sigma]_{\theta=\pi/2 - \pi/N} = r_0\sin\sigma_i/\sin(\sigma_i + \pi/N) \qquad (7.e)$$

but also from the geometry (Figure (2.b))

$$r_0 = \tan\sigma\sin\theta + \frac{\tan\sigma\cos\theta}{\tan\sigma_i}$$

implying

$$\tan\sigma_i = \frac{\sin(\pi/N)\tan\delta - \tan\delta\cos\theta}{\cos(\pi/N)\tan\delta + \tan\sigma\sin\theta}$$

Substituting for $\tan\sigma_i$ in Equation (6.e), it can be shown that $(W/V_n)_b = \cot(\sigma_i - \theta)/\cos\sigma_b$ which is exactly the inner boundary condition at off design condition (Appendix (A)). Also, looking at Equations (5.e), it is seen that at $\theta = \pi/2 - \pi/N$, $W = 0$, i.e. at symmetry line, but from Equations (5.e):

$$(W)_{\theta=\pi/2} \neq 0 \qquad (\partial V_n/\partial\theta)_{\theta=\pi/2-\pi/N} = 0 \qquad (\partial V_n/\partial\theta)_{\theta=\pi/2} \neq 0$$

$\sigma_i = 30°$, $r_0 = 0.5$

$\theta°$	$\sigma°$	$(W/V_n)_b$
43	14.4	4.5
45	14.5	3.85
50	14.85	2.85
60	16.1	1.8
0	18.07	1.15
80	21.3	0.9
90	26.6	0.64

$\sigma_i = 20°$, $r_0 = 0.5$

$\theta°$	$\sigma°$	$(W/V_n)_b$
25	9.74	11.6
30	9.85	5.75
40	10.3	2.8
50	11.17	1.76
60	12.6	1.22
70	14.5	0.87
80	18.8	0.61
90	26.6	0.4

$\sigma_i = 10°$, $r_0 = 0.5$

$\theta°$	$\sigma°$	$(W/V_n)_b$
13	4.96	19.15
18	5	7.14
20	5.05	5.7
30	5.3	2.8
40	5.7	1.74
45	6.05	1.43
50	6.47	1.19
60	7.7	0.84
70	9.9	0.585
80	14.24	0.88
90	26.6	0.2

$\sigma_i = 2°$, $r_0 = 0.5$

$\theta°$	$\sigma°$	$(W/V_n)_b$
5	1	19
10	1	7
15	1.02	4.33
20	1.05	3.07
30	1.132	1.85
45	1.36	1.07
50	1.69	0.9
60	1.88	0.623
70	2.66	0.4
80	4.79	0.21
90	26.5	0.09

Table (1). Tables of $(W/V_n)_b$ for various "σ_i" for N = 4 and $r_0 = 0.5$

$\sigma_i=30°$, $r_0=0.1$

$\theta°$	$\sigma°$	$(W/V_n)_b$
33	26.59	21.33
40	27	6.36
45	27.3	4.202
50	28	3.112
60	30	2
70	33.13	1.413
80	37.87	1.063
90	45	0.816

$\sigma_i=20°$, $r_0=0.1$

$\theta°$	$\sigma°$	$(W/V_n)_b$
25	18.9	12
30	19.2	6
40	20	3
45	20.6	2.3
50	21.55	1.86
60	24.06	1.305
70	28	0.95
80	34.3	0.7
90	45	0.515

$\sigma_i=10°$, $r_0=0.1$

$\theta°$	$\sigma°$	$(W/V_n)_b$
15	19.8	11.6
20	10	5.75
30	10.66	2.78
40	11.33	1.77
50	12.77	1.23
60	15.117	0.87
70	19.15	0.612
80	26.2	0.4
90	45	0.24

$\sigma_i=2°$, $r_0=0.1$

$\theta°$	$\sigma°$	$(W/V_n)_b$
10	2	7.11
20	2.1	3.079
30	2.26	1.88
40	2.5	1.28
50	2.98	0.901
60	3.76	0.62
70	5.3	0.41
80	9.5	0.22
90	45	0.45

Table (2). Tables of $(W/V_n)_b$ for various geometry for $N = 4$ and $r_0 = 0.1$.

$\theta_s = 20°$ N = 4

M_∞	$\sigma_i°$	r_0	r_L/r_s	r_s	$\bar{W}$	$\bar{V}_n$	r_1
1.6054	22.12	0.6	1.41	12.56	$\bar{W}_1$	$\bar{V}_{n1}$	0.245
1.6054	22.12	0.6	1.42	1.21	$\bar{W}_2$	$\bar{V}_{n2}$	0.245
1.6054	61.72	0.4	1.03	17.8	$\bar{W}_1$	$\bar{V}_{n1}$	1.03
1.6054	45	0.456	1.36	13.95	$\bar{W}_1$	$\bar{V}_{n1}$	0.322
1.8714	45	0.456	1.15	1.0315	$\bar{W}_1$	$\bar{V}_{n1}$	0.322
1.8714	45	0.456	1.475	0.84	$\bar{W}_1$	$\bar{V}_{n1}$	0.521

Table (3). Table of M_∞, σ_i, r_0, r_L/r_s, r_i in Case (1).

$\theta_s = 20°$, $\theta^* = 65°$, N = 4

M_∞	σ_i°	r_0	r_L/r_s	r_s	r_i
1.6054	22.12	0.6	2.59	0.245	6.69
1.6531	22.12	0.6	1.286	0.205	0.913
1.8714	22.12	0.6	1.3	0.245	0.772
1.8714	45	0.456	1.24	0.373	0.815
1.8714	61.7	0.4	1.03	0.367	0.845
2.129	22.12	0.6	1.27	0.245	0.679

Table (4). Table of M_∞, σ_1, r_0, r_L/r_s, r_s for $\theta_s = 20°$ and $\theta^* = 65°$ in Case (2).

$\theta^* = 65°, \quad \theta_s = 30°, \quad N = 4$

M_∞	σ_i	r_0	r_L/r_s	r_i	r_s
1.82	61.7	0.635	1.06	0.583	1.275
1.82	45	0.723	1.18	0.511	1.2
1.82	22.12	0.9517	1.67	0.388	1.12

Table (5). Table of M_∞, σ_i, r_0, r_L/r_s, r_s for $\theta_s = 30°$ $\theta^* = 65°$ in Case (2).

$\theta = 20°$ $N = 4$

M_∞	$\sigma_i°$	r_0	r_L/r_s	r_i	$\theta*°$	r_s
1.6531	22.12	0.6	1.33	0.243	73	0.913
1.8714	22.12	0.6	1.43	0.245	73	0.708
1.8714	45	0.456	1.135	0.33	73	0.795
1.8714	61.7	0.4	1.03	0.36	76	0.836
2.129	22.12	0.6	1.43	0.245	73	0.637
1.8714	22.12	0.6	1.35	0.245	50	0.824
2.129	22.12	0.6	2.75	0.245	50	0.7133

Table (6). Table of M_∞, σ_i, r_0, r_L/r_s, r_s for $\theta_s = 20°$, $\theta* = 73°$ and $76°$ in Case (2).

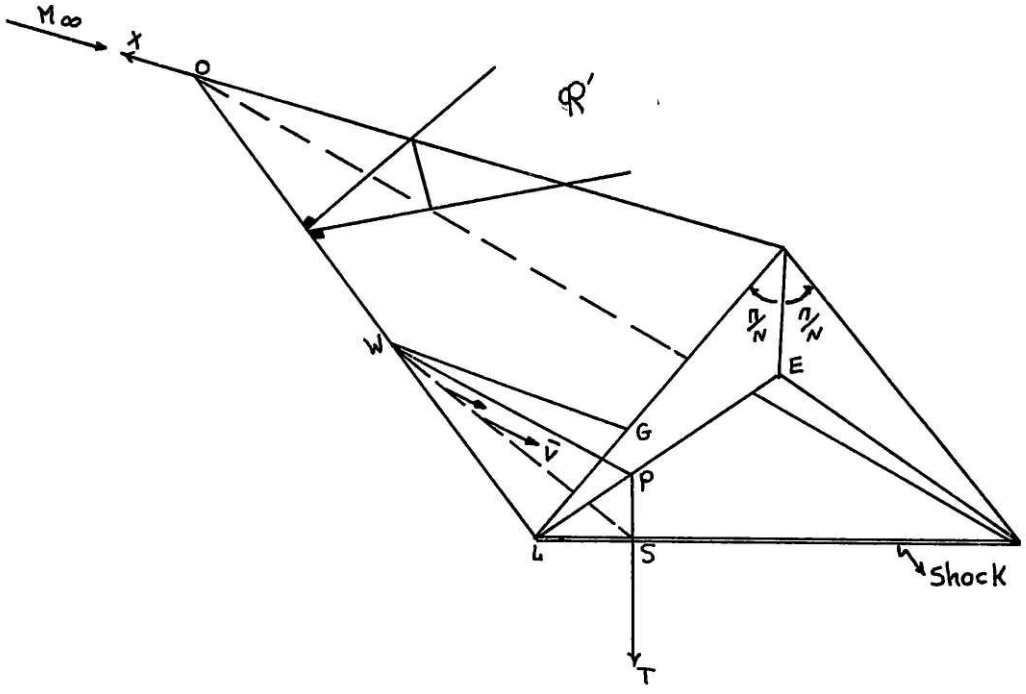

Figure (1). Wave rider on design

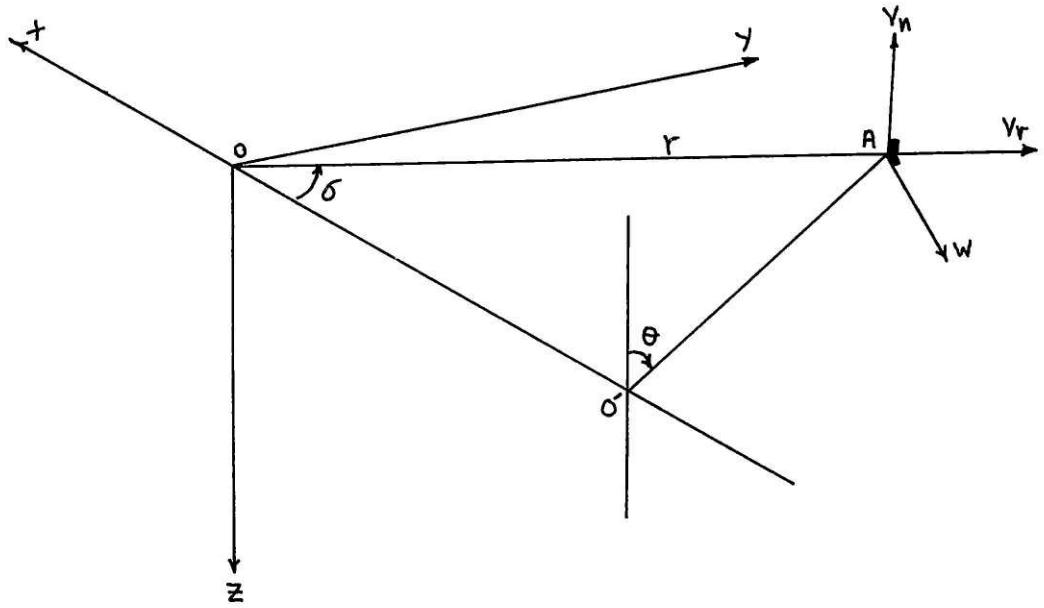

Figure (2a) Three dimensional veiw of the spherical coordinates.

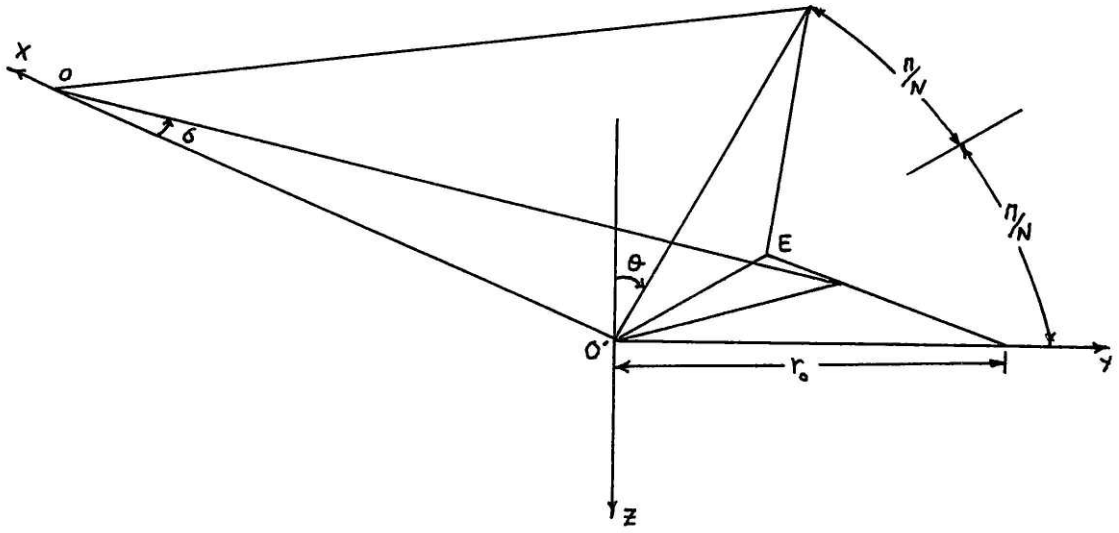

Figure (2b). Three dimensional view of the body, with indicated geometry parameters.

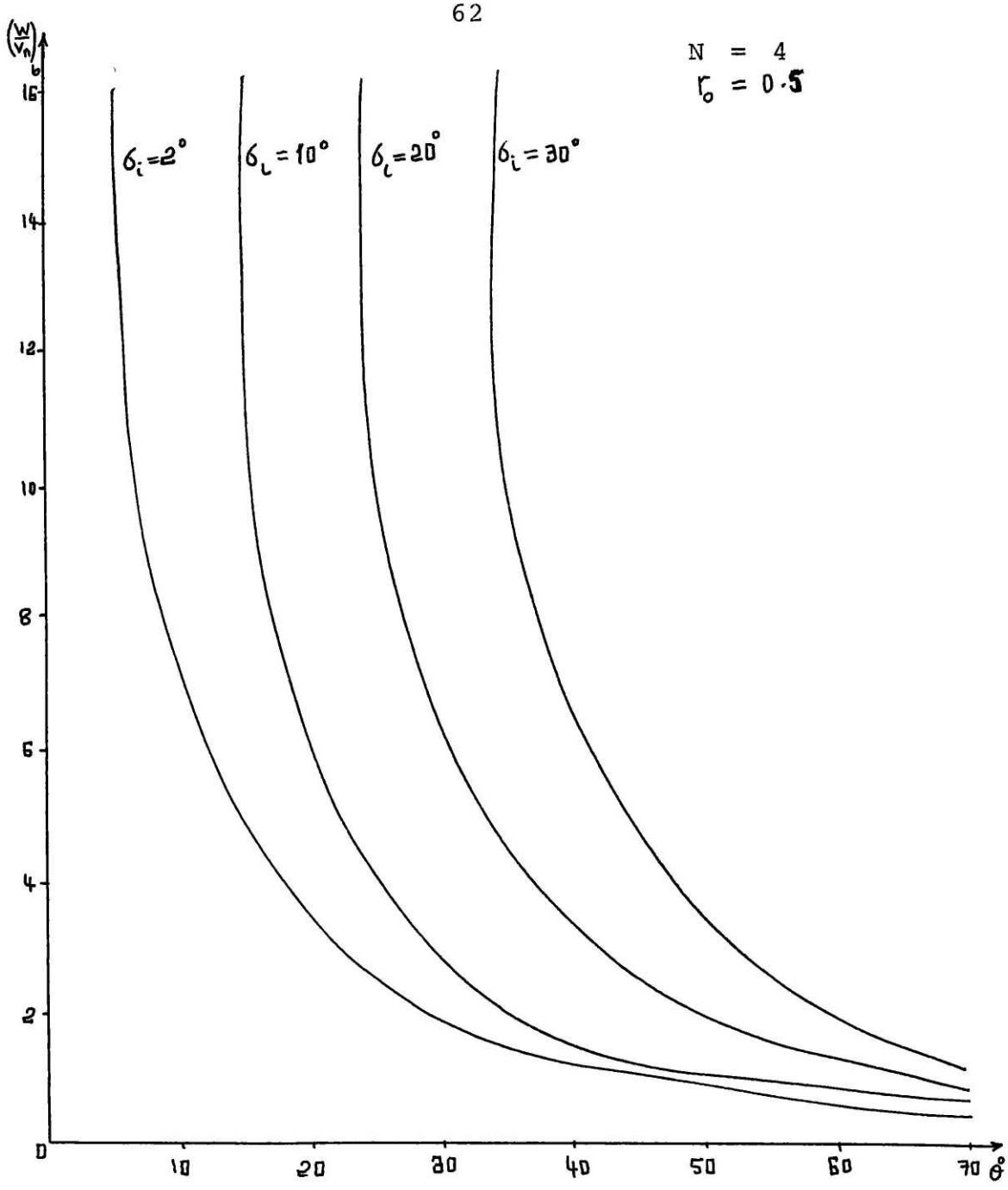

Figure (3a). $(W/V_n)_b$ curves for various body geometry.

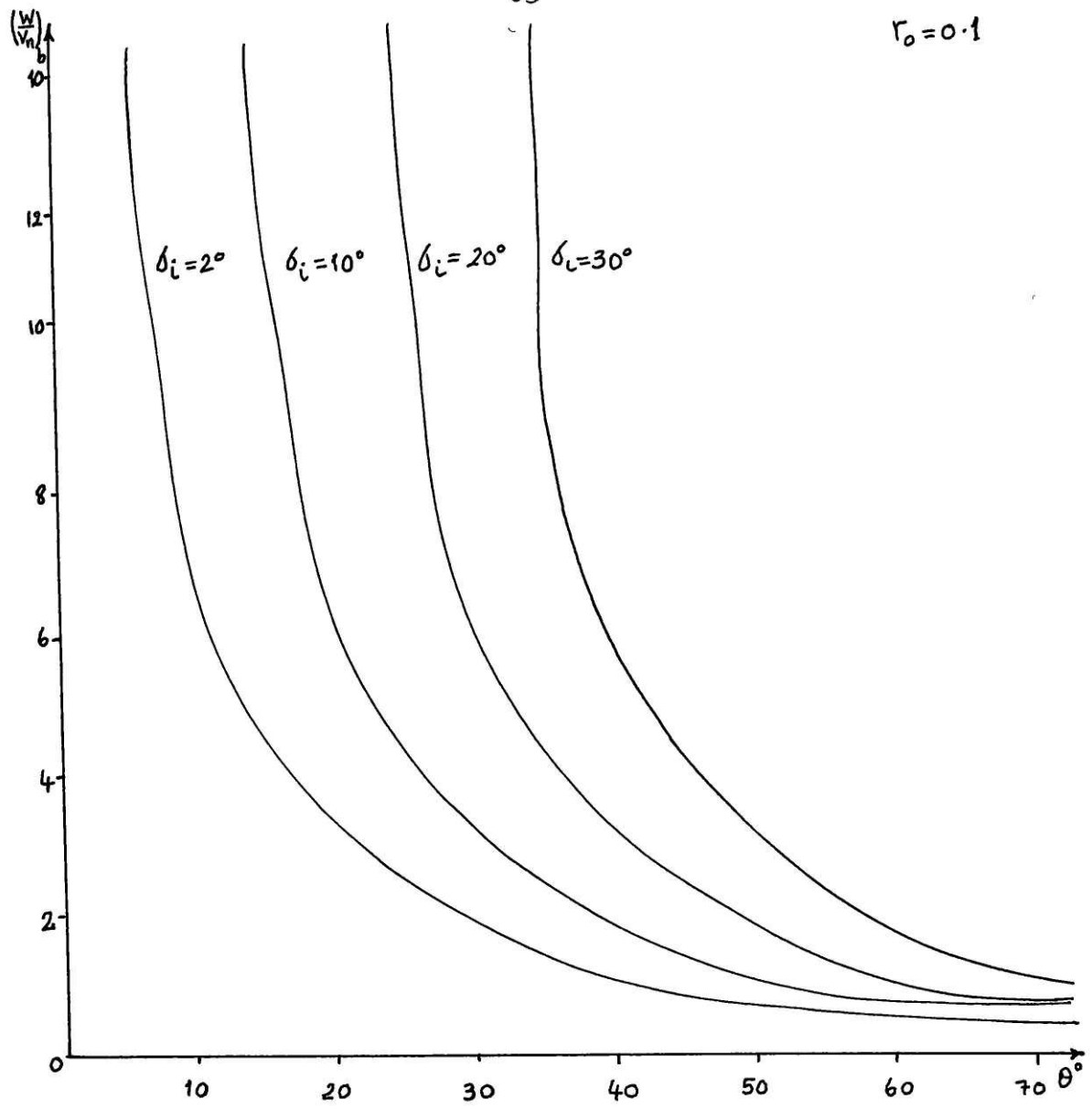

Figure (3b). $(W/V_n)_b$ curves for various body geometry, for N = 4 and r_0 = 0.1.

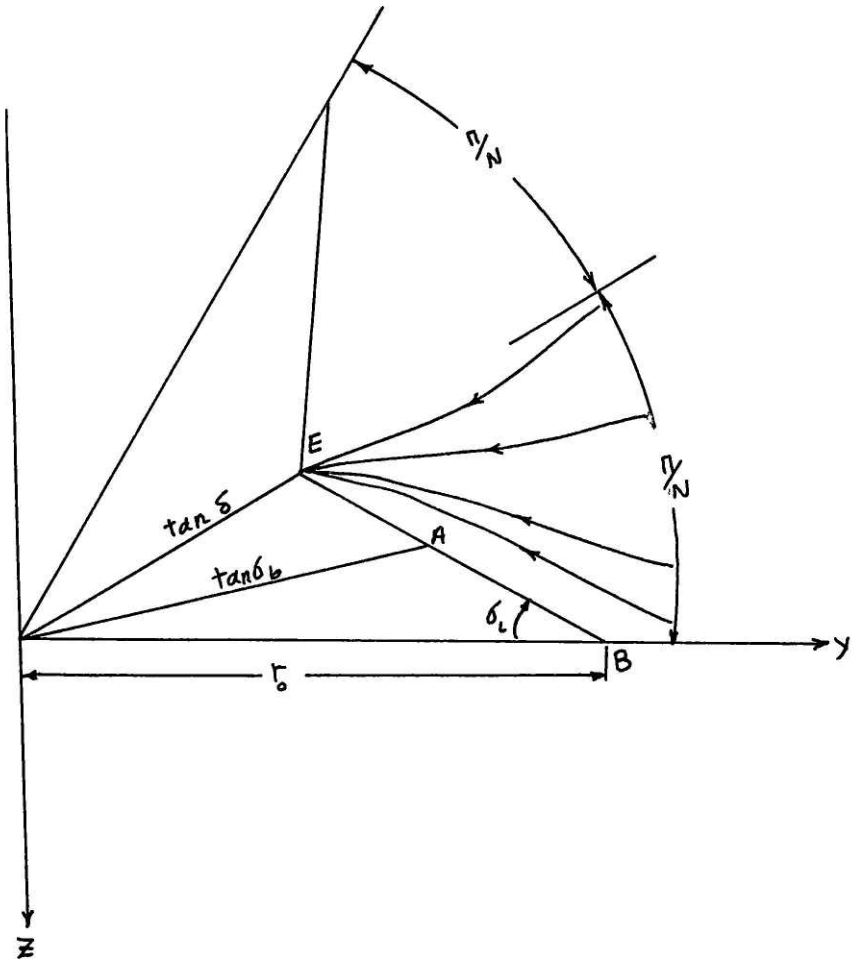

Figure (4a). Cross sectional view of the assumed flow for the wave rider in Case (2).

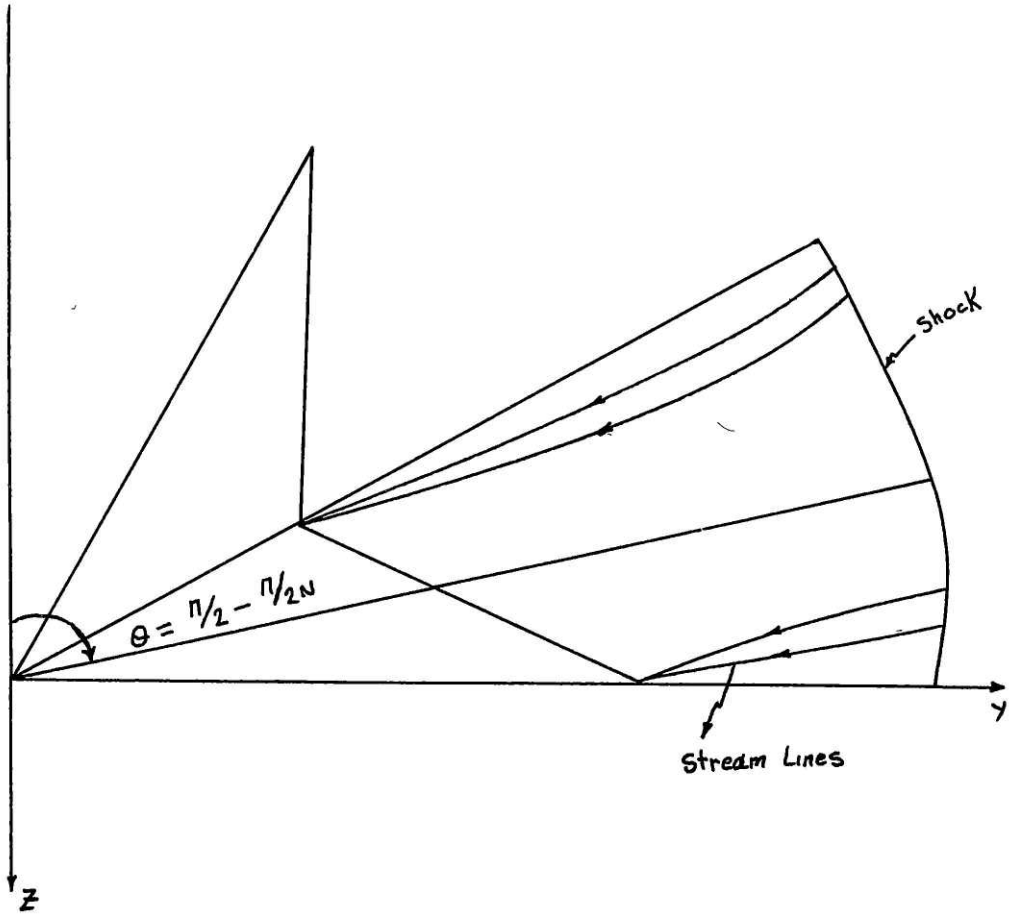

Figure (4b). Cross sectional view of the assumed flow for Case (3).

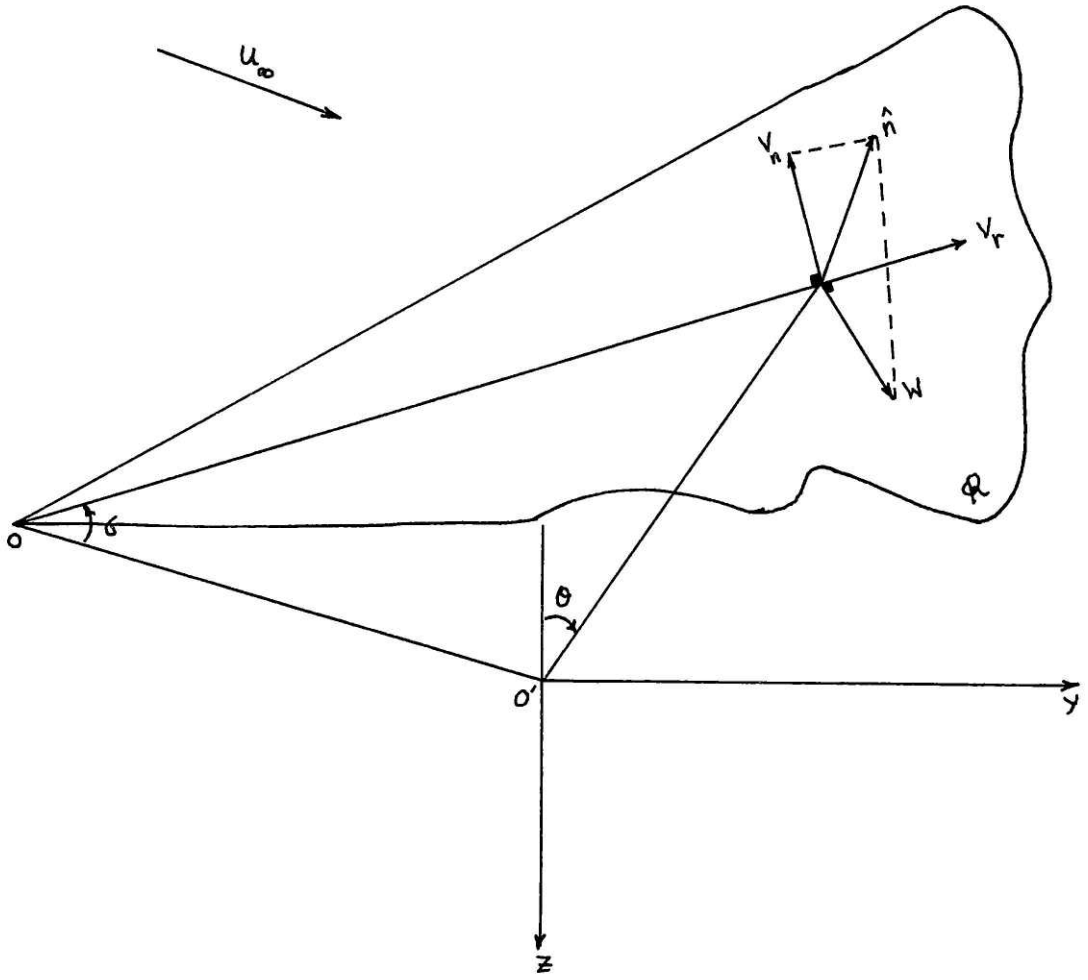

Figure (5). Three dimensional view of a conical shock, with specified spherical coordinates.

	σ_i°	r_0	M_∞	N		
– – – –	22.12	0.6	1.6054	4	$\bar{W}_2$	$\bar{V}_{n2}$
————	61.7	0.4	1.6054	4	$\bar{W}_2$	$\bar{V}_{n2}$

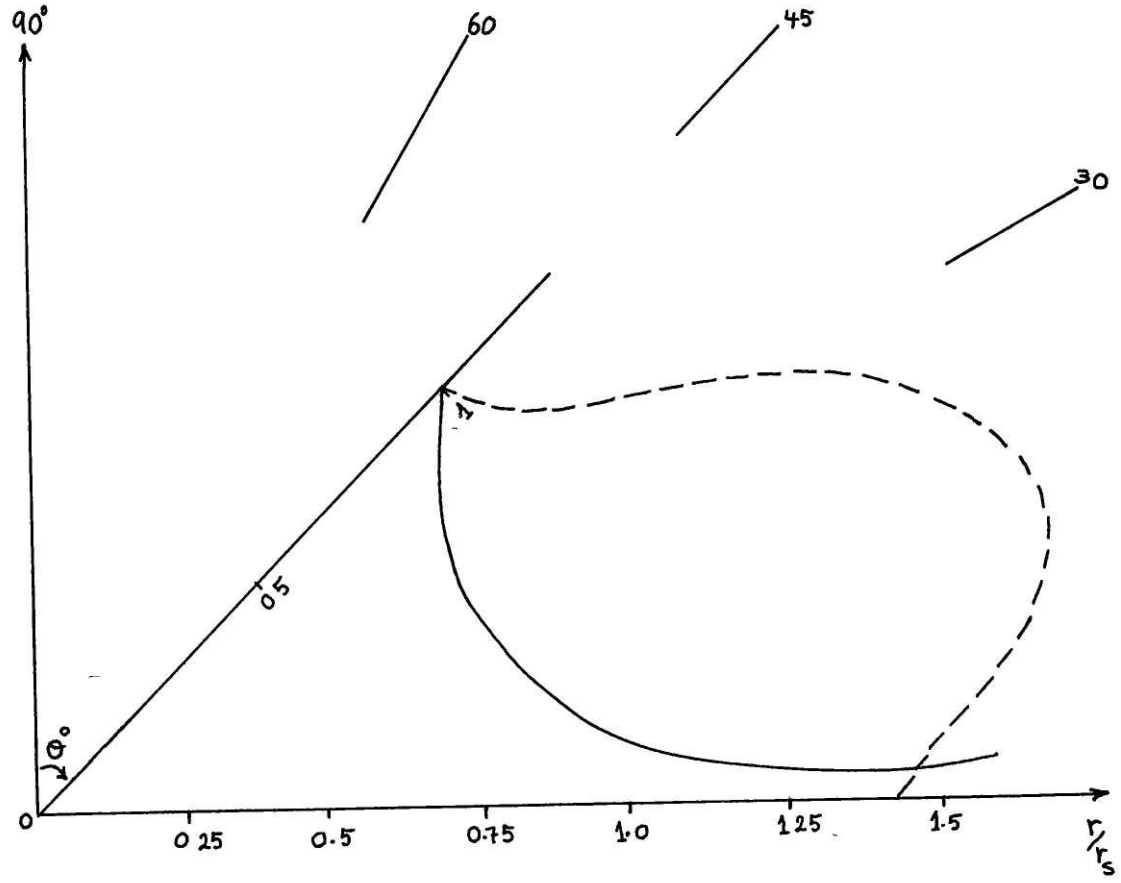

Figure (6). Shock shapes for Case (1), at constant $M_\infty = 1.6054$.

	σ_i	r_0	M_∞	N		
—·— —	45°	0.456	1.8714	4	$\bar{W}_2$	$\bar{V}_{n2}$
- - - - - -	45°	0.456	1.8714	4	W_1	V_{n1}
———	45°	0.456	1.6054	4	$\bar{W}_1$	V_{n1}

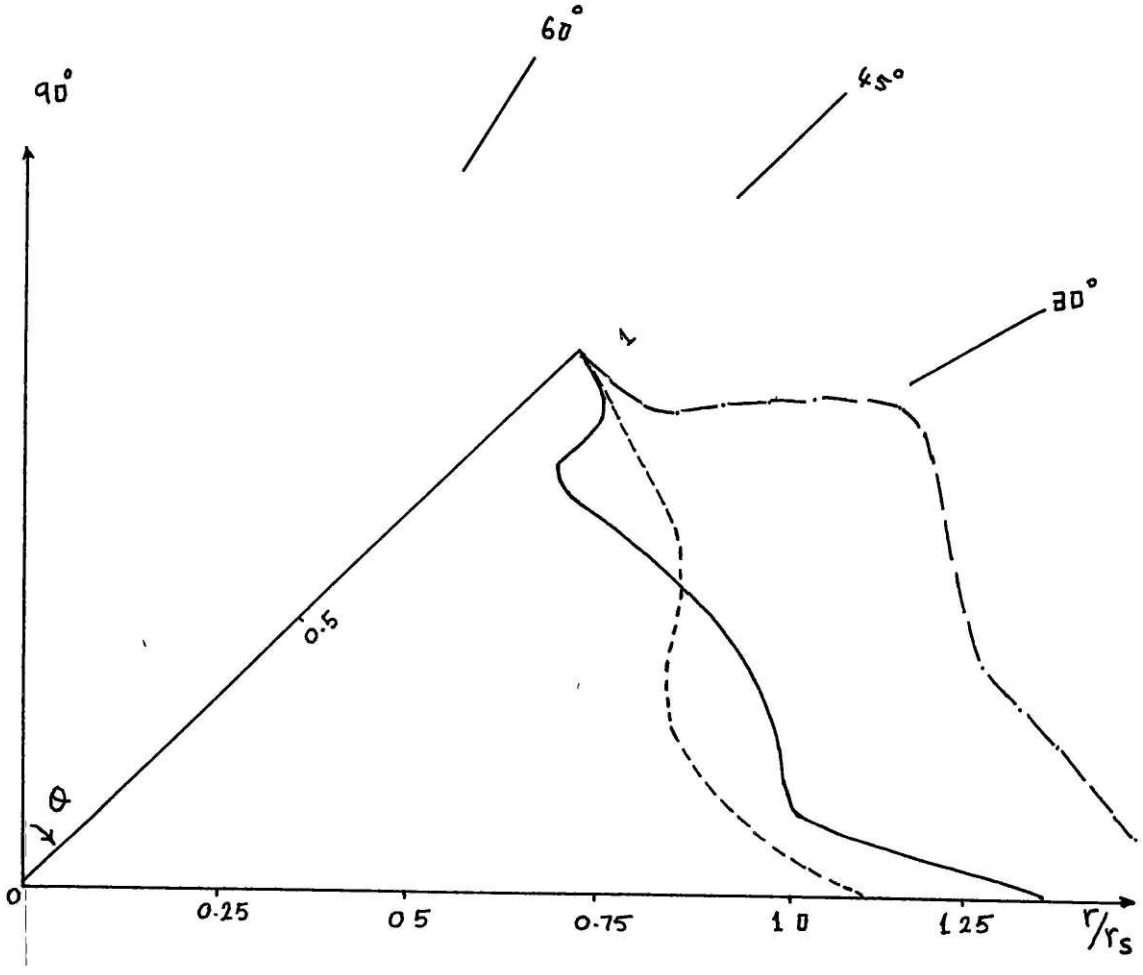

Figure (7). Shock shapes for a fixed geometry in Case (1).

	σ_i°	r_0	M_∞	N	θ_s°	$\theta^{*\circ}$
-------	22.12	0.6	1.6054	4	20	65
-.-.-.-	22.12	0.6	1.6531	4	20	65
- - - -	22.12	0.6	1.8714	4	20	65
———	22.129	0.6	2.129	4	20	65

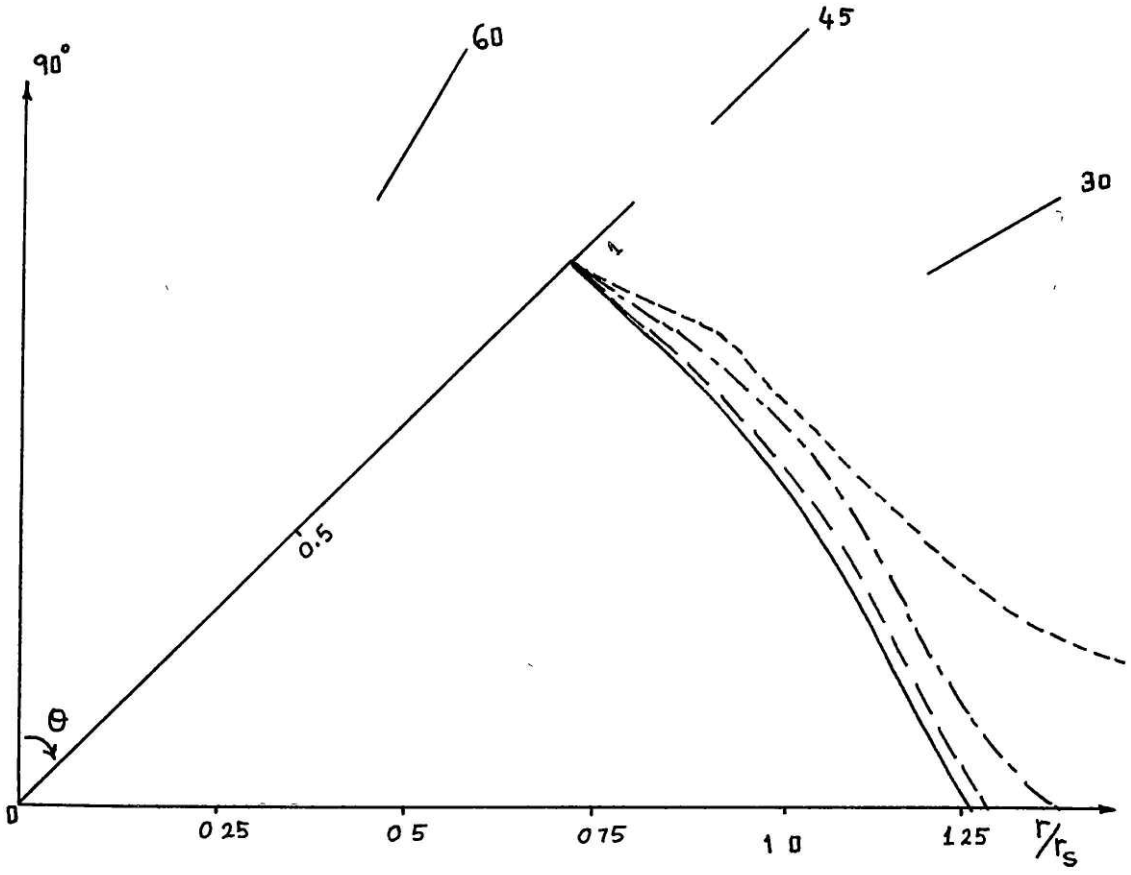

Figure (8). Shock shapes for a fixed geometry, with $\theta_s = 20°$ and $\theta^* = 65°$ in Case (2).

	σ_i	r_0	M_∞	N	θ_s°	$\theta^{*\circ}$
————	22.12	0.6	1.8714	4	20	65
— — — —	22.12	0.456	1.8714	4	20	65
- - - - -	22.12	0.4	1.8714	4	20	65

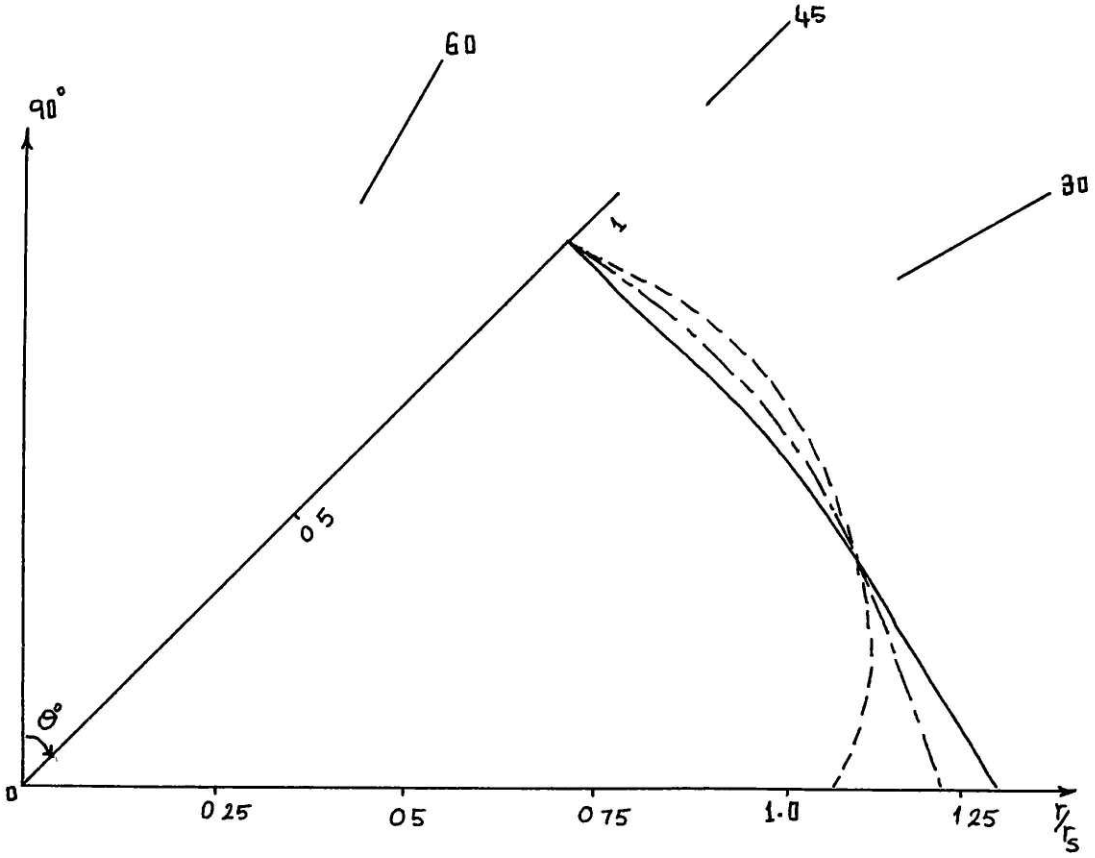

Figure (9). Shock shapes at constant $M_\infty = 1.8714$, for $\theta_s = 20°$ and $\theta^* = 65°$ in Case (2).

	σ_i	r_0	M_∞	N	θ_s°	$\theta^{*\circ}$
– – – –	61.7	0.4	1.8714	4	20	65
————	45	0.456	1.8714	4	20	65
–.–.–.–	22.12	0.6	1.8714	4	20	65

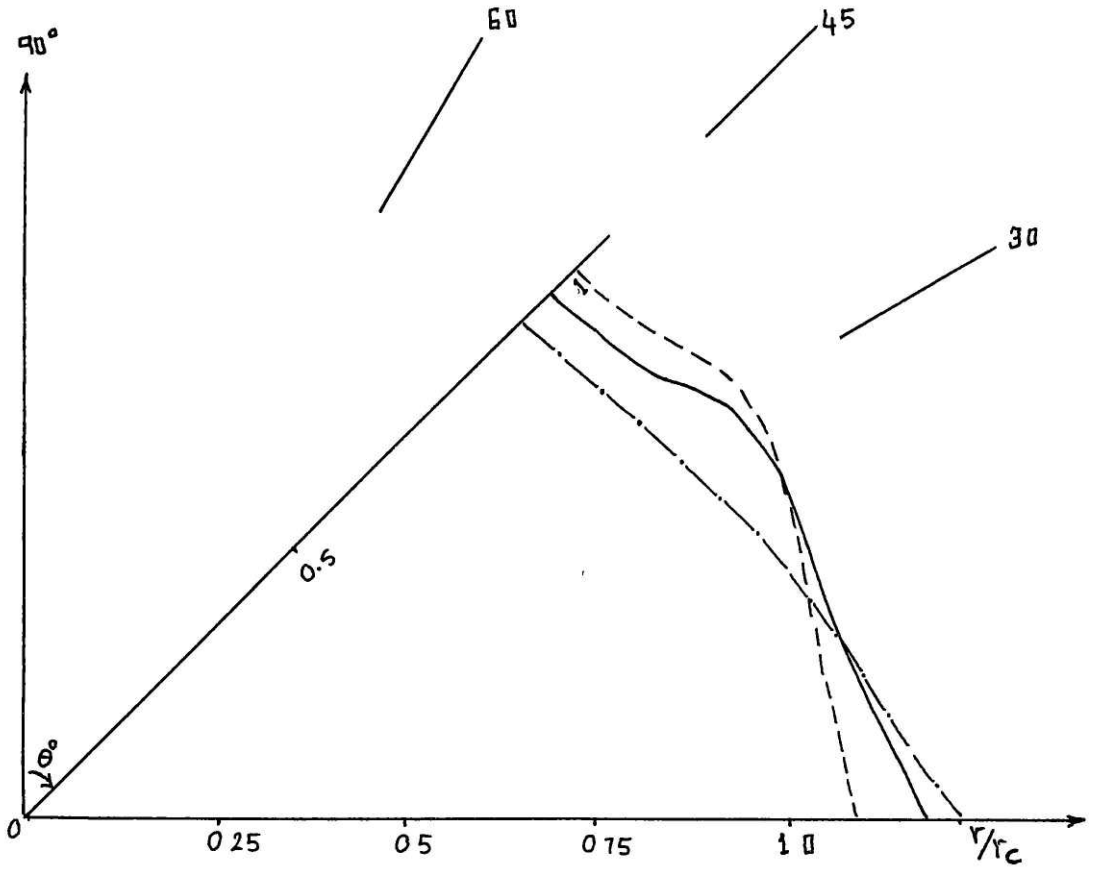

Figure (10). Shock shapes relative to equivalent cone shock at constant $M_\infty = 1.8714$, with $\theta_s = 20°$ and $\theta^* = 65°$ in Case (2).

	σ_i°	r_0	M_∞	θ_s°	$\theta^{*\circ}$
————	45	0.723	1.82	30	65
—.—.—.—.—.—	61.7	0.635	1.82	30	65
— — — — — —	22.12	0.952	1.82	30	65

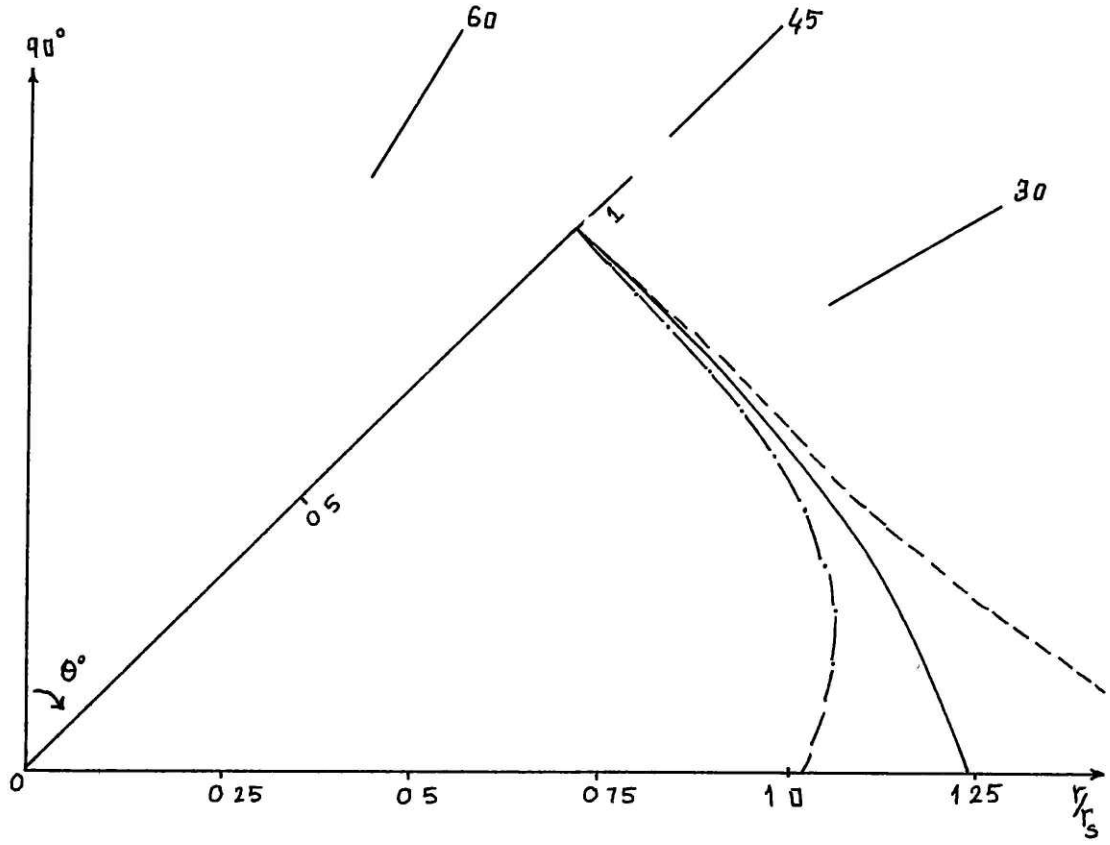

Figure (11). Shock shapes at constant $M_\infty = 1.82$, for $\theta_s = 30°$ and $\theta^* = 65°$ in Case (2).

	σ_i	r_0	M_∞	N	θ_s°	$\theta^{*\circ}$
-------	22.12	0.6	2.1297	4	20	73
———	22.12	0.6	1.653	4	20	73
– – – – –	22.12	0.6	1.8714	4	20	73

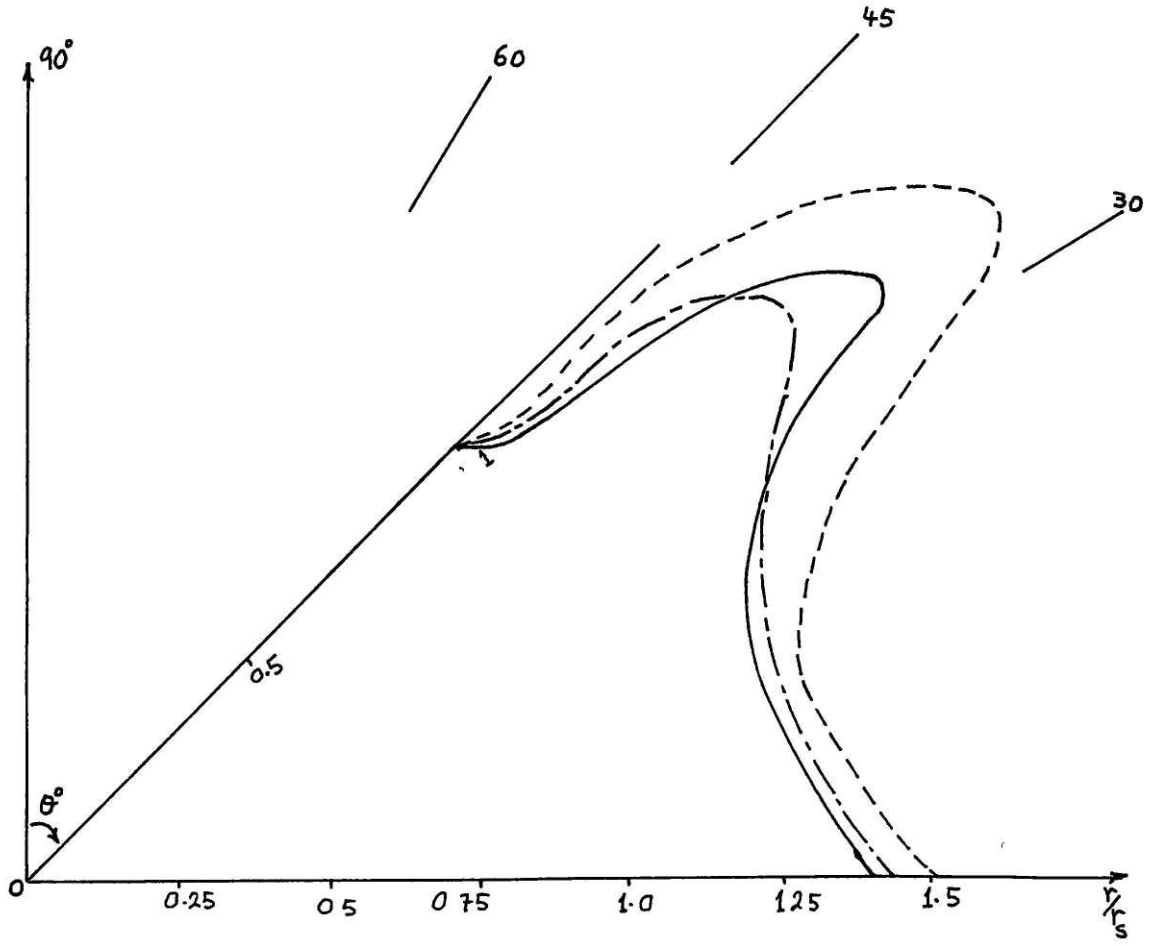

Figure (12). Shock shapes for fixed geometry, for $\theta_s = 20°$ and $\theta^* = 73°$ in Case (2).

	σ_i°	r_0	M_∞	N	θ_s°	$\theta^{*\circ}$
– – – – –	61.7	0.4	1.8714	4	20	76
————	45	0.456	1.8714	4	20	73
---------	22.12	0.6	1.8714	4	20	73

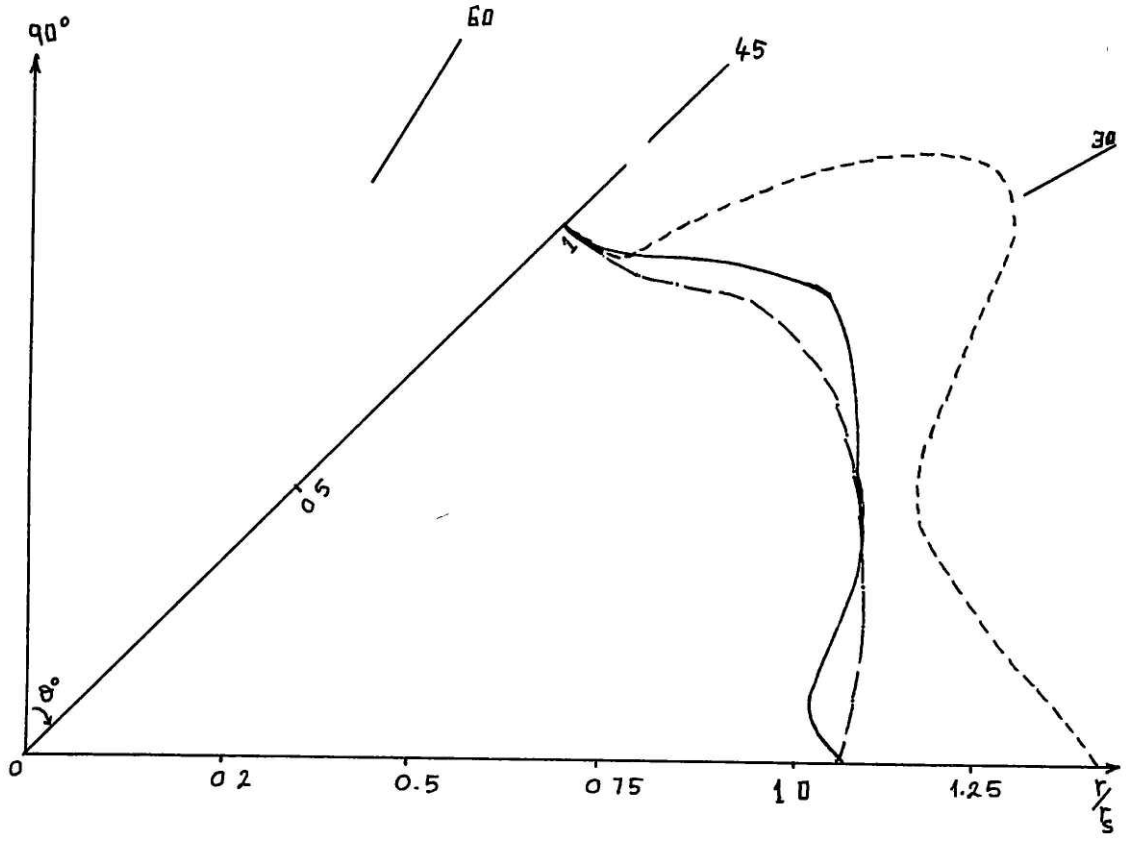

Figure (13). Shock shapes at constant $M_\infty = 1.8714$, for $\theta_s = 20°$ and $\theta^* = 73°$ and $76°$ in Case (2).

	σ_i°	r_0	M_∞	N	θ_s°	$\theta^{*\circ}$
– – – – – –	22.12	0.6	2.129	4	50	20
————	22.12	0.6	1.8714	4	50	20

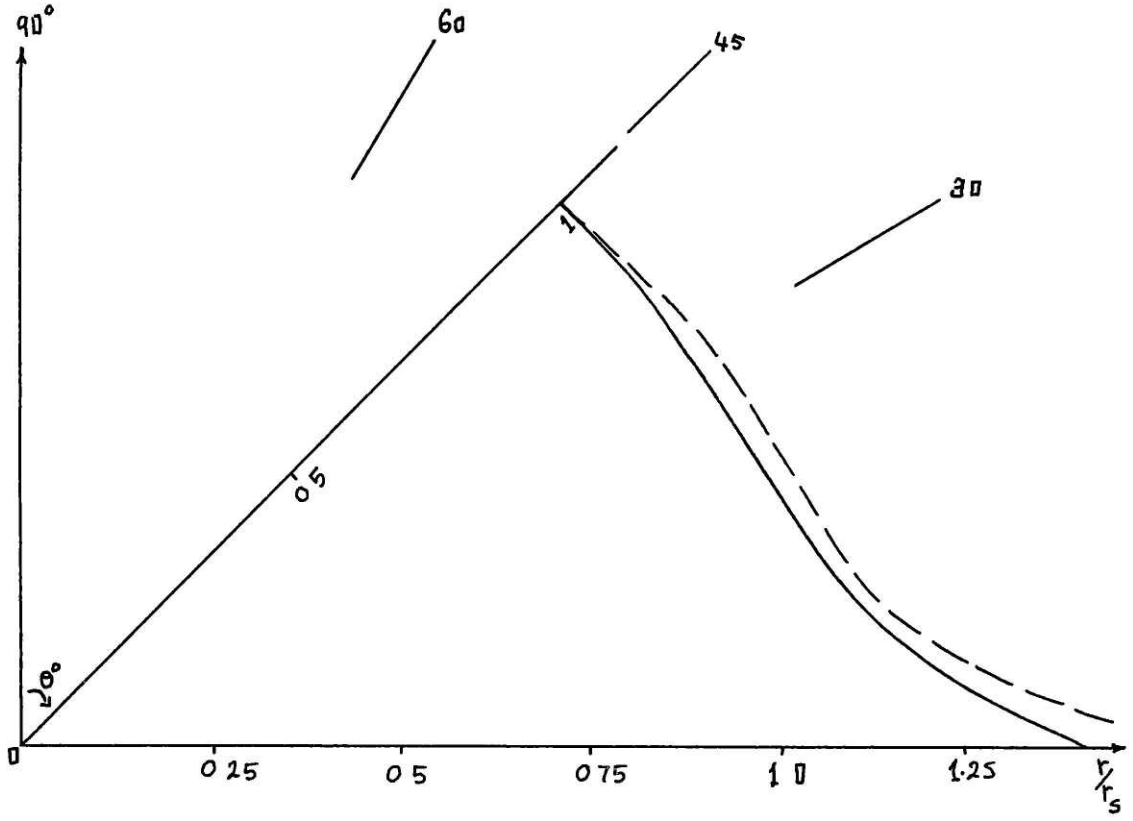

Figure (14). Shock shapes for fixed geometry, with $\theta_s = 20°$ and $\theta^* = 50°$ in Case (2).

REFERENCES

1 Maikapar, G.I., "On the wave drag of non-anisymmetric bodies at supersonic speeds", P.M.M. Vol. 23, No. 2, 1959, 376-378.

2 Nonweiler, T., "Delta wings of shapes amenable to exact shock wave theory", Journal of the Royal Aeronautical Society, Vol. 67, 1959, 39-40.

3 Maikapar, G.I., "Bodies formed by the stream surfaces of conical flows", Fluid Dynamics, Vol. 1, No. 1, 1966, 89-90.

4 Kopal, Z., "Tables of supersonic flow around cones", MIT Technical Report No. 1, 1947.

5 Sears, W.R.(Ed), General Theory of High Speed Aerodynamics, Princeton Series, Volume 6, 722-740. New Jersey: Princeton University Press.